Received: 13 February 2019 | Revised: 14 May 2019 | Accepted: 20 May 2019

DOI: 10.1111/bph.14762

RESEARCH PAPER

# Endothelial TRPV4 channels modulate vascular tone by $Ca^{2+}$-induced $Ca^{2+}$ release at inositol 1,4,5-trisphosphate receptors

Helen R. Heathcote[1] | Matthew D. Lee[1] | Xun Zhang[1] | Christopher D. Saunter[2] | Calum Wilson[1] | John G. McCarron[1]

[1] Strathclyde Institute of Pharmacy and Biomedical Science, University of Strathclyde, Glasgow, UK

[2] Centre for Advanced Instrumentation, Biophysical Sciences Institute, Department of Physics, Durham University, Durham, UK

**Correspondence**
John G. McCarron, Strathclyde Institute of Pharmacy and Biomedical Science, University of Strathclyde, 161 Cathedral Street, Glasgow G4 0RE, UK.
Email: john.mccarron@strath.ac.uk

**Funding information**
British Heart Foundation, Grant/Award Numbers: PG/16/54/32230 and PG16/82/32439; Wellcome Trust, Grant/Award Numbers: 202924/Z/16/Z and 204682/Z/16/Z

**Background and Purpose:** The TRPV4 ion channels are $Ca^{2+}$ permeable, non-selective cation channels that mediate large, but highly localized, $Ca^{2+}$ signals in the endothelium. The mechanisms that permit highly localized $Ca^{2+}$ changes to evoke cell-wide activity are incompletely understood. Here, we tested the hypothesis that TRPV4-mediated $Ca^{2+}$ influx activates $Ca^{2+}$ release from internal $Ca^{2+}$ stores to generate widespread effects.

**Experimental Approach:** $Ca^{2+}$ signals in large numbers (~100) of endothelial cells in intact arteries were imaged and analysed separately.

**Key Results:** Responses to the TRPV4 channel agonist GSK1016790A were heterogeneous across the endothelium. In activated cells, $Ca^{2+}$ responses comprised localized $Ca^{2+}$ changes leading to slow, persistent, global increases in $Ca^{2+}$ followed by large propagating $Ca^{2+}$ waves that moved within and between cells. To examine the mechanisms underlying each component, we developed methods to separate slow persistent $Ca^{2+}$ rise from the propagating $Ca^{2+}$ waves in each cell. TRPV4-mediated $Ca^{2+}$ entry was required for the slow persistent global rise and propagating $Ca^{2+}$ signals. The propagating waves were inhibited by depleting internal $Ca^{2+}$ stores, inhibiting PLC or blocking $IP_3$ receptors. $Ca^{2+}$ release from stores was tightly controlled by TRPV4-mediated $Ca^{2+}$ influx and ceased when influx was terminated. Furthermore, $Ca^{2+}$ release from internal stores was essential for TRPV4-mediated control of vascular tone.

**Conclusions and Implications:** $Ca^{2+}$ influx via TRPV4 channels is amplified by $Ca^{2+}$-induced $Ca^{2+}$ release acting at $IP_3$ receptors to generate propagating $Ca^{2+}$ waves and provide a large-scale endothelial communication system. TRPV4-mediated control of vascular tone requires $Ca^{2+}$ release from the internal store.

**Abbreviations:** 2-APB, 2-aminoethoxydiphenyl borate; CPA, cyclopiazonic acid; F, fluorescence intensity; $F_0$, baseline fluorescence intensity; GSK, GSK1016790A; HC067, HC067047; $IP_3$, inositol 1,4,5-trisphosphate; $IP_3R$, inositol 1,4,5-trisphosphate receptor; RuR, ruthenium red; RyRs, ryanodine receptors; SNP, sodium nitroprusside

## 1 | INTRODUCTION

The endothelium plays a critical role in the regulation of numerous vascular processes such as maintaining vascular tone, regulating the passage of macromolecules and oxygen to tissues, modulating immune responses, initiating angiogenesis, and controlling vascular remodelling. The control by the endothelium of each process is mediated by the generation of various signalling molecules that include NO, prostacyclin, von Willebrand factor, tissue plasminogen activator, and endothelial-derived hyperpolarizing and contracting factors (Taylor et al., 2003; Whorton, Willis, Kent, & Young, 1984). The generation of each of these signalling molecules is controlled tightly by changes in the cytoplasmic $Ca^{2+}$ concentration in the endothelium. Central therefore to an understanding of endothelial function is an appreciation of the control of intracellular $Ca^{2+}$ concentrations.

There are two major sources of $Ca^{2+}$ for the endothelium: the extracellular space and the intracellular $Ca^{2+}$ store. $Ca^{2+}$ influx from the extracellular space is mediated mainly by channels present on the plasmalemmal membrane. In many cell types, such as smooth muscle and cardiomyocytes, the influx pathways are well characterized, and **voltage-dependent $Ca^{2+}$ channels** are major contributors (Catterall, 2011; Nelson, Patlak, Worley, & Standen, 1990). In endothelial cells, however, understanding of the $Ca^{2+}$ influx pathways is incomplete (Nilius, Droogmans, & Wondergem, 2003). Several members of the transient receptor potential (TRP) superfamily of cation channels are present in endothelial cells (Hofmann, Schaefer, Schultz, & Gudermann, 2002; Nilius, Droogmans, & Wondergem, 2003). Of these, the **TRPV4** channel has attracted substantial interest because of the channels' relatively high $Ca^{2+}$ permeability (Filosa, Yao, & Rath, 2013; Watanabe et al., 2002). TRPV4 channels are expressed widely in endothelial cells (Mendoza et al., 2010; Sullivan, Francis, Pitts, Taylor, & Earley, 2012; Watanabe et al., 2002). TRPV4 channels were initially demonstrated to be activated by hypotonicity-induced cell swelling (Liedtke et al., 2000; Mizuno, Matsumoto, Imai, & Suzuki, 2003). Later studies revealed that the channel is also activated by various other stimuli including mechanical stimulation (Gao, Wu, & O'Neil, 2003; Kohler et al., 2006; Liedtke, Tobin, Bargmann, & Friedman, 2003), moderate heat, endogenous chemicals such as **anandamide**, **arachidonic acid**, and its epoxyeicosatrienoic acid metabolites, as well as by a number of exogenous chemical ligands (Nilius & Voets, 2013; Vriens et al., 2004; Watanabe et al., 2003) or UVB (Moore et al., 2013; Yin et al., 2008). In the endothelium, by regulating the cytoplasmic $Ca^{2+}$ concentration, TRPV4 channels may contribute to the response to arachidonic acid metabolites, physical forces, and agonists (Bagher et al., 2012; Freichel et al., 2001; Hartmannsgruber et al., 2007; Kohler et al., 2006; Marrelli, O'Neil, Brown, & Bryan, 2007; Mendoza et al., 2010; Watanabe et al., 2002; Zhang et al., 2009; Zhang, Papadopoulos, & Hamel, 2013).

While large in amplitude, the $Ca^{2+}$ rise evoked by activation of endothelial TRPV4 channels is reported to be highly localized and confined to within a few micrometres of the channels (Sonkusare et al., 2012; Sonkusare et al., 2014). These highly localized $Ca^{2+}$ signals evoke endothelial and smooth muscle hyperpolarization and vascular relaxation (F. Gao & Wang, 2010; Kohler et al., 2006; Ma et al., 2013; Sonkusare et al., 2012; D. X. Zhang et al., 2009). The highly localized nature of the $Ca^{2+}$ signal provides tight spatial control of the cellular effectors activated, for example, **$Ca^{2+}$-activated $K^+$ channels** (Gao & Wang, 2010; Ma et al., 2013; Sonkusare et al., 2012). However, more widespread $Ca^{2+}$ rises throughout the cytoplasm have been implicated in the regulation of endothelial structure, maintenance of the normal orientation of endothelial cells, the control and selectively of endothelial permeability, and the production of antithrombotic factors. TRPV4 channels have been proposed to play a role in each of these processes (Noren et al., 2016; Phuong et al., 2017; Thodeti et al., 2009; Thoppil et al., 2016). The question arises as to how activation of TRPV4 channels may lead to $Ca^{2+}$-dependent events throughout the cytoplasm if the increase in $Ca^{2+}$ concentration arising from TRPV4 channel activity remains localized to within a few microns of the channel.

The second major source of $Ca^{2+}$ in endothelial cells is the internal $Ca^{2+}$ store. $Ca^{2+}$ release from the internal store may occur via **ryanodine** receptors (**RyRs**) or **$IP_3$** receptors (**$IP_3$Rs**). While RyRs may be expressed in endothelial cells (Moccia, Berra-Romani, & Tanzi, 2012; Mumtaz, Burdyga, Borisova, Wray, & Burdyga, 2011; Rusko, Wang, & Vanbreemen, 1995), the functional role of the channels in the endothelium is not clear given that RyR activators such as **caffeine** do not increase cytoplasmic $Ca^{2+}$ in endothelial cells (Borisova, Wray, Eisner, & Burdyga, 2009; Wilson et al., 2019; Wilson, Lee, & McCarron, 2016). $Ca^{2+}$ release from the internal store in endothelial cells may be mediated mainly by $IP_3$Rs (Mumtaz et al., 2011; Wilson

### What is already known

- TRPV4 channels are key $Ca^{2+}$ permeable channels that control endothelial function.
- TRPV4 channels generate large but highly localized $Ca^{2+}$ signals.

### What this study adds

- $Ca^{2+}$-induced $Ca^{2+}$ release from $IP_3$-sensitive internal store amplifies local $Ca^{2+}$ signals from TRPV4 channel activity.
- $Ca^{2+}$-induced $Ca^{2+}$ release at $IP_3$ receptors mediates control of vascular contractility by endothelial TRPV4 channels.

### What is the clinical significance

- Endothelial TRPV4 channels are involved in several disease conditions such as cancer progression and hypertension.
- Endothelial TRPV4-mediated $Ca^{2+}$-induced $Ca^{2+}$ release at $IP_3$ receptors offers a new target for drug development.

et al., 2019). $Ca^{2+}$ release via $IP_3R$ occurs in response to physical forces and circulating vasoactive substances and contributes to the control of several vascular activities such as vasorelaxation, endothelial permeability, and production of anti-thrombotic factors (Sun, Geyer, & Komarova, 2017).

$IP_3Rs$ are themselves regulated by $Ca^{2+}$, in addition to $IP_3$. $Ca^{2+}$ released via $IP_3Rs$ may induce a positive feedback $Ca^{2+}$-induced $Ca^{2+}$ release process at neighbouring $IP_3Rs$. Indeed, $Ca^{2+}$ signals at $IP_3Rs$ begin as a localized $Ca^{2+}$ blip at a single receptor (~1 μm spread) which expand by $Ca^{2+}$-induced $Ca^{2+}$ release opening neighbouring $IP_3Rs$ generating a $Ca^{2+}$ puff (~4 μm spread). Puffs may further propagate via $Ca^{2+}$-induced $Ca^{2+}$ release to form a transient global $Ca^{2+}$ elevation throughout the cell or a $Ca^{2+}$ "wave" (Berridge, 1997; Bootman, Niggli, Berridge, & Lipp, 1997). These waves may move through all or part of the cell (Bootman, Berridge, & Lipp, 1997). In some conditions that are not fully understood, $IP_3$-evoked $Ca^{2+}$ waves may also move between cells to provide a signalling system capable of coordinating the activity of many cells (Leybaert & Sanderson, 2012).

While $Ca^{2+}$ influx and release are activated separately, they are not independent: $Ca^{2+}$ influx can trigger release, and release can trigger influx (McCarron, Chalmers, Bradley, Macmillan, & Muir, 2006). In cardiomyocytes, $Ca^{2+}$ influx via voltage-dependent $Ca^{2+}$ channels may activate RyRs to evoke a large rise in $Ca^{2+}$, inducing cell contraction. In smooth muscle cells, TRPV4 channel activity may lead to $Ca^{2+}$-induced $Ca^{2+}$ release acting at RyRs (Earley, Heppner, Nelson, & Brayden, 2005). In astrocytes, $Ca^{2+}$-induced $Ca^{2+}$ release occurs in response to $Ca^{2+}$ influx via TRPV4 channels but at $IP_3Rs$ rather than at RyRs. This process amplifies and propagates the $Ca^{2+}$ signal arising from TRPV4-mediated $Ca^{2+}$ influx (Dunn, Hill-Eubanks, Liedtke, & Nelson, 2013). TRPV4-mediated $Ca^{2+}$ influx may also lead to recruitment of $IP_3Rs$ and $Ca^{2+}$-induced $Ca^{2+}$ release in murine-derived cultured neuronal cells (Shen et al., 2018). These observations raise the possibility of TRPV4-mediated $Ca^{2+}$ influx being able to generate a more global increase in intracellular $Ca^{2+}$ via $Ca^{2+}$-induced $Ca^{2+}$ release in endothelial cells.

To explore this possibility, we examined the role that the internal store plays in regulating alterations in intracellular $Ca^{2+}$ evoked by activation of TRPV4 channels. Here, we report that the $IP_3$-sensitive $Ca^{2+}$ store is critical for the TRPV4-evoked global $Ca^{2+}$ rise in endothelial cells in intact blood vessels. $Ca^{2+}$ influx generates $Ca^{2+}$-induced $Ca^{2+}$ release at $IP_3Rs$ to evoke $Ca^{2+}$ waves in the vascular endothelium. $IP_3R$-dependent $Ca^{2+}$ waves are required for the endothelium-dependent vascular smooth muscle cell relaxation in response to activation of TRPV4 channels.

## 2 | METHODS

### 2.1 | Animals

All animal care and experimental procedures complied with the relevant UK Home Office Regulations, (Schedule 1 of the Animals [Scientific Procedures] Act 1986, UK) and were approved by the University of Strathclyde Animal Welfare and Ethical Review Body. Animal studies are reported in compliance with the ARRIVE guidelines (Kilkenny et al., 2010) and with the recommendations made by the *British Journal of Pharmacology*. The Strathclyde Biological Protection Unit is a conventional unit which undertakes FELASA quarterly health monitoring. Male Sprague–Dawley rats (10–12 week old; 250–300 g), from an in-house colony, were used for the study. Sprague–Dawley rats are a widely used experimental model with a wealth of background information to aid interpretation of results. The animals were housed three per cage, and the cage type was North Kent Plastic model RC2F with nesting material "Sizzle Nest." A 12:12 light dark cycle was used with a temperature range of 19–23°C (set point 21°C) and humidity levels between 45% and 65%. Animals had free access to fresh water and SDS diet RM1 (rodent maintenance). The enrichment in the cages was aspen wood chew sticks and hanging huts.

All experiments used first- or second-order mesenteric arteries isolated from rats killed by either $CO_2$ or by injection with pentobarbital; no differences in the results were observed with either method. Controls and experimental treatments were carried out in the same tissue, so blinding and randomization were not used.

### 2.2 | High-resolution imaging of endothelial $Ca^{2+}$ signalling

Arteries (diameter of 200–230 μm) were isolated from the mesenteric bed, cleaned, then cut and pinned flat *en face* (endothelial side facing up) on a Sylgard block. The endothelium was then preferentially loaded with Cal-520/AM (5 μM; with 0.02% Pluronic F-127) in physiological saline solution (PSS) at 37°C for 30 min (Wilson, Lee, & McCarron, 2016; Wilson, Saunter, Girkin, & McCarron, 2016). Following incubation, arteries were gently washed with PSS, and the Sylgard blocks were placed face down on a custom flow chamber. Arteries were then continuously perfused with PSS at 1.5 $ml \cdot min^{-1}$ using a syringe pump. Endothelial $Ca^{2+}$ activity was stimulated by swapping the PSS syringe for one containing **ACh** (100 nM) or **GSK1016790A** (GSK, 20 nM). GSK1016790A is a selective TRPV4 channel agonist and evokes $Ca^{2+}$ influx in wild type but not TRPV4 channel knockout mice (Mannaa et al., 2018; Sonkusare et al., 2012).

In experiments examining the effects of various pharmacological agents on stimulated endothelial $Ca^{2+}$ signalling, drugs were added to the perfusate and remained thereafter. Images were acquired at 10 Hz using an inverted fluorescence microscope (Eclipse TE300, Nikon, Tokyo, Japan) equipped with a 40× objective (S Fluor, Nikon, Tokyo, Japan, NA = 1.3) and an electron-multiplying charge-coupled device camera (iXon Life; Andor Technology Limited, Belfast, Northern Ireland, UK) or on an upright epi-fluorescence microscope (FN-1, Nikon, Tokyo, Japan) equipped with a 60× objective (CFI Fluor, Nikon, Tokyo, Japan, NA = 1.0). Cal520/AM was excited at 488 nm using a monochrometer (Polychome IV, TILL Photonics,

Graefelfing, Germany) or an LED illumination system (PE-300Ultra, CoolLED, Andover, UK).

In some experiments, the endothelium was loaded with Cal-520 (5 μM) and a membrane permeant, caged $IP_3$ (5 μM), and the $Ca^{2+}$ response to local photolysis of caged $IP_3$ examined. In these experiments, the endothelium was imaged as above, and a xenon flash lamp (Rapp Optoelecktronic, Germany) was used to uncage $IP_3$ (Olson, Chalmers, & McCarron, 2012; Olson, Sandison, Chalmers, & McCarron, 2012; Wilson et al., 2019).

## 2.3 | Extraction and analysis of endothelial $Ca^{2+}$ signals

Endothelial $Ca^{2+}$ signals were extracted automatically from fluorescence recordings using custom written Python software (RRID: SCR_001658; Lee et al., 2018; Wilson, Lee, & McCarron, 2016; Wilson, Saunter, et al., 2016). In brief, cellular regions of interest (ROIs) were first generated from average-intensity projections of each time series recording. Intensity projections were sharpened (un-sharp mask filter) and thresholded, generating ROIs that encompassed the majority of each cell's area. To facilitate comparisons in paired experiments, for example, where $Ca^{2+}$ activity was recorded before and after pharmacological inhibition, ROIs were aligned and tracked across separate image acquisitions. Only cells that remained within the field of view for all recordings were included.

Cellular $Ca^{2+}$ signals were extracted by averaging fluorescence intensity within each of the ROIs, for each frame of the image stack. Raw fluorescence signals (F) were expressed as fractional changes in fluorescence intensity ($F/F_0$) by dividing each intensity value by the average intensity of a 100-frame period exhibiting the least activity/noise ($F_0$, red in Figure S1B). The $F_0$ period was determined automatically by calculating, in series, the derivative of the signal, the rolling (100-frame) SD of the derivative, and the rolling (100-frame) summation of the rolling SD. The minimum value of the rolling summation indicates the centre of the portion of the signal with the least activity/noise.

The $Ca^{2+}$ response to activation of TRPV4 channels contained two main components: a "slow" persistent $Ca^{2+}$ elevation rise in the baseline $Ca^{2+}$ levels and fast intracellular $Ca^{2+}$ waves. To determine the underlying mechanisms, we isolated the two components from each $F/F_0$ trace. The slow persistent $Ca^{2+}$ elevation (baseline) component of each signal was extracted by applying an asymmetric least squares (ALS) smoothing function (Figure S1C–E; Eilers & Boelens, 2005). Signalling metrics describing this slow persistent $Ca^{2+}$ elevation (amplitude; time of activation, 10–90% rise time) were then calculated from a fitted sigmoidal curve (Figure S1C–E). Cells were considered to exhibit a persistent $Ca^{2+}$ elevation if the slow $F/F_0$ component rose by more than 10-fold the SD of the baseline noise. The propagating $Ca^{2+}$ wave (fast) component of each signal was extracted by dividing each $F/F_0$ trace by the ALS-smoothed signal. This procedure effectively flattens the baseline and removes any slow drift from the signal (Figure S1C–E). Peaks in each $Ca^{2+}$ signal arising from the waves were then detected automatically, using a zero-crossing detector on derivative $F/F_0$ traces (Lee et al., 2018; Wilson, Lee, & McCarron, 2016). Various signal metrics (number of peaks, peak amplitudes, peak durations, 10–90% rise time, and 90–10% fall time) were extracted from the corresponding ALS-smoothed $F/F_0$ trace. Cells were considered to exhibit $Ca^{2+}$ wave activity if the $F/F_0$ component exhibited at least one event with an amplitude more than 10-fold the SD of the baseline noise.

In some experiments, $Ca^{2+}$ signals were calibrated using $\left[Ca^{2+}\right] = K_D \frac{F - F_{min}}{F_{max} - F}$, where $K_D$ = 320 nM. $F_{max}$ was determined at the end of the experiment by the addition of ionomycin (1 μM) and $F_{min}$ the signal in the absence of light to the camera.

## 2.4 | Measurement of vascular reactivity

To assess the endothelium dependence of contractile and dilation responses, vascular reactivity to various agonists were assessed in *en face* artery preparations. This technique permits simultaneous visualization of the endothelium and assessment of functional responses (contraction and dilation) and was used so that we could confirm the removal of the endothelium as required.

Arteries of 200–230 μm diameter were loaded with Cal-520/AM as above, except that they were pinned to the bottom of a custom, Sylgard-coated flow chamber. This flow chamber was designed to facilitate the perfusion of solutions (1.5 ml·min$^{-1}$) when mounted on an upright microscope (FN-1, Nikon, Tokyo, Japan). Handling and pinning of the arteries were restricted to the outermost corners, leaving the central portion of the vessels with intact endothelium and able to contract/dilate freely.

Following incubation, arteries were gently washed with PSS and left to equilibrate for 30 min in PSS (continuously perfused 1.5 ml·min$^{-1}$ using a syringe pump). Contraction was stimulated by swapping the PSS for one containing **phenylephrine**. The concentration of phenylephrine was titrated to contract arteries to ~20% of resting diameter. Relaxation was stimulated by changing the phenylephrine-containing syringe for one containing phenylephrine (at the same concentration) and either ACh (100 nM), GSK1016790A (GSK, 20 nM), or **sodium nitroprusside** (SNP, 100 μM). Contractile and dilator responses were assessed before and after (paired) various treatments in the same artery, as described in the text. After treatment, antagonists were continuously present in the PSS. The removal of the endothelium was achieved by gentle mechanical disruption with a human hair that was superglued onto a pipette tip. Endothelium removal was confirmed by the absence of endothelial cells stained with the $Ca^{2+}$ indicator Cal-520/AM. After the removal of the endothelium, arteries were left to equilibrate for 60 min.

Images were acquired at 10 or 5 Hz (consistent within each experimental protocol) using an upright fluorescence microscope equipped with a 16× objective lens (0.8 NA; Nikon, Tokyo, Japan) and large

format (1,024 × 1,024; 13-μm pixels) back-illuminated electron-multiplying charge-coupled device camera (iXon 888; Andor, Belfast, UK) and stored for offline analysis. An edge-detection algorithm (Lawton et al., 2019) was used to track the width of arteries in image recordings. The algorithm extracts an intensity profile along a scanline orientated perpendicular to the longitudinal axis of the vessel. Each intensity profile was smoothed using a 251-point, fifth-order Savitzky–Golay filter, and the first-order derivative calculated. The edges of the artery correspond to the maxima and minima of the first-order derivative, which were identified and tracked using a zero-crossing detector. The width of the artery equates to the unfolded circumference of the intact vessel and was converted to the equivalent diameter. To control for variation in the resting diameters, summary contractile response data are expressed as the percentage reduction from resting diameter,while relaxation responses are expressed as the percentage increase in diameter compared to resting diameter (Figure S2).

## 2.5 | Matching arterial tone across experimental conditions

Following the removal of the endothelium, arteries were significantly more sensitive to phenylephrine. The concentration of phenylephrine was titrated to achieve a level of tone that was comparable to that achieved in the presence of a functional endothelium (Figure S2A). In the presence of **cyclopiazonic acid** (CPA), Phenylephrine-induced contractions were transient, and it was not possible to achieve a stable contraction. Therefore, assessing the effect of store depletion on TRPV4-induced dilation was not feasible. Instead, vessels were pretreated with GSK and CPA, and the magnitude of the transient contraction induced by phenylephrine was assessed. Furthermore, after depletion of $Ca^{2+}$ stores using CPA, a significantly higher concentration of phenylephrine was required to generate comparable levels of vascular tone (Figure S2B).

## 2.6 | Pressure myography

Diameter measurements of pressurized arteries were performed using the VasoTracker open source pressure myograph system (system (RRID:SCR_017233; Lawton et al., 2019). Mesenteric arteries were dissected free from surrounding tissue, cleaned of connective tissue, and mounted on similar sized glass pipettes in a VasoTracker pressure myograph chamber. Arteries were pressurized to 70 mmHg, checked for leaks, and left to equilibrate for 30 min in pre-warmed (37°C) circulating PSS, with intraluminal flow (~100 μl·min$^{-1}$) established by a 10 cm$H_2O$ pressure gradient.

Artery diameter was monitored using an sCMOS camera (DCC1545M, Thorlabs, New Jersey, USA) and recorded by VasoTracker acquisition software. Arteries were contracted using phenylephrine (~500 nM) to ~80% of resting diameter, which was added to the perfusion solution. All other drugs (e.g., ACh and GSK) were applied intraluminally. Summary relaxation data are expressed as the percentage increase in diameter compared to resting diameter.

## 2.7 | Materials

Cal-520/AM was obtained from Abcam (Cambridge, MA, USA). Caged-$IP_3$ (caged-$IP_3$ 4,5-dimethoxy-2-nitrobenzyl) was obtained from Sichem (Germany). Pluronic F-127 was obtained from Invitrogen (Carlsbad, CA, USA). U73343 was obtained from Tocris (St Louis, MO, USA). All other drugs and chemicals were obtained from Sigma (St Louis, MO, USA). GSK, **HC067047**, CPA, **U73122**, U73343, **2-aminoethoxydiphenyl borate** (2-APB), and ionomycin were dissolved in DMSO and diluted to working concentration in PSS such that the total volume of DMSO was less than or equal to 0.1%. All other drug stocks were dissolved in water. The PSS consisted of the following (mM): 145 NaCl, 4.7 KCl, 2.0 MOPS, 1.2 $NaH_2PO_4$, 5.0 glucose, 0.02 EDTA, 1.17 $MgCl_2$, and 2.0 $CaCl_2$ (adjusted to pH 7.4 with NaOH). In experiments using a $Ca^{2+}$-free PSS, $Ca^{2+}$ was substituted with $Mg^{2+}$ on an equimolar basis, and EGTA (1 mM) was included. All solutions were freshly prepared each day.

## 2.8 | Data and statistical analysis

The data and statistical analysis in this study comply with the recommendations of the British Journal of Pharmacology on experimental design and analysis in pharmacology The *n* vales shown are the numbers of biological replicates (number of animals). For each replicate, a single field of endothelial cells ($Ca^{2+}$ imaging experiments) or a single artery segment (vascular reactivity studies) was studied. Summary data are presented graphically as paired mean responses, or as the grand mean ± SEM of *n* biological replicates. Two-tailed, paired t test (for paired observations), independent two-sample *t* tests or repeated measures one-way ANOVA with multiple comparisons were used as indicated in the text. All statistical analyses were performed using GraphPad Prism version 6.0 (RRID:SCR_002798; GraphPad Software, La Jolla, CA, USA). A *P* value of <.05 was considered statistically significant.

## 2.9 | Nomenclature of targets and ligands

Key protein targets and ligands in this article are hyperlinked to corresponding entries in http://www.guidetopharmacology.org, the common portal for data from the IUPHAR/BPS Guide to PHARMACOLOGY (Harding et al., 2018), and are permanently archived in the Concise Guide to PHARMACOLOGY 2017/18 (Alexander, Christopoulos et al., 2017; Alexander, Fabbro et al., 2017; Alexander, Peters et al., 2017; Alexander, Striessnig et al., 2017).

## 3 | RESULTS

### 3.1 | Characteristics of ACh- and GSK-evoked $Ca^{2+}$ signals

To determine if activation of TRPV4 channels in endothelial cells evoked $Ca^{2+}$ release from the internal store, endothelial cells were loaded with the fluorescent $Ca^{2+}$ indicator Cal520/AM and activated with ACh (100 nM) or the TRPV4 channel agonist GSK (20 nM). $Ca^{2+}$ activity was then visualized in the fields of ~100 endothelial cells. Cellular responses were analysed individually (Figures 1 and S1).

$Ca^{2+}$ responses evoked by ACh and GSK were clearly different (Figure 1). ACh evoked a rapid elevation in intracellular $Ca^{2+}$ which was followed by asynchronous oscillations across the field of view (Figure 1; Mumtaz et al., 2011). Activation of TRPV4 channels resulted in heterogeneous $Ca^{2+}$ responses (Figure 1c, Movie S1, and Figure S3) that consisted of several distinct phases (Figures 1 and 2).

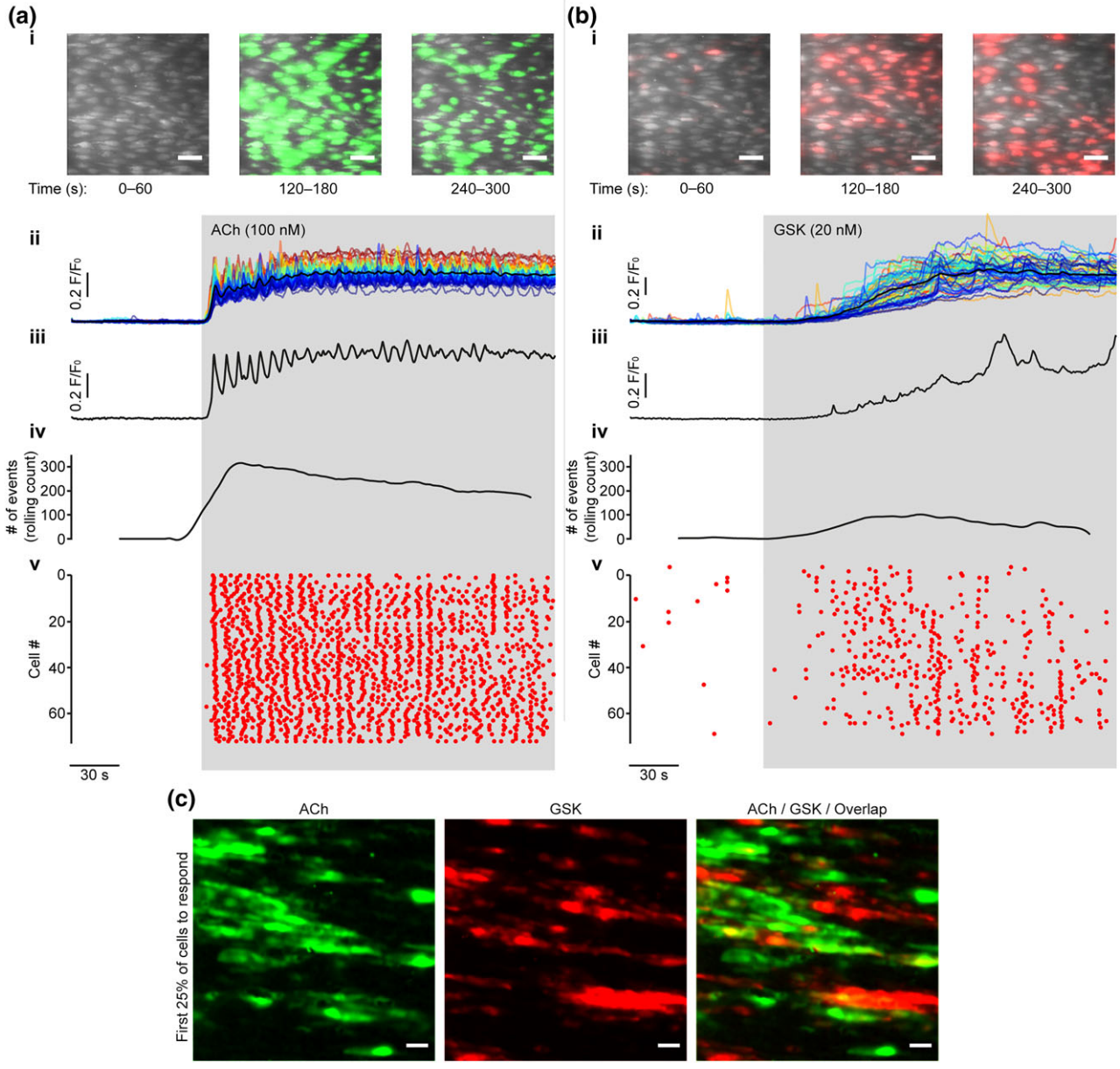


**FIGURE 1** ACh and GSK1016790A stimulate different $Ca^{2+}$ signalling patterns. (a, b) $Ca^{2+}$ dynamics visualized in a single *en face* endothelial preparation stimulated with ACh (a), and GSK1016790A (GSK, b). Panels show: (i) composite images illustrating endothelial $Ca^{2+}$ activity over the time course of the experiment, scale bars = 50 μm; (ii) whole-cell $Ca^{2+}$ traces ($F/F_0$) for all cells shown in the corresponding panel in (i) ranked and coloured according to the magnitude of the signal (dark blue, low; dark red, high); (iii) a representative $Ca^{2+}$ trace from a single cell; (iv) a rolling summation (30 s) of the number of $Ca^{2+}$ events (peaks) across the-field of-view; and (v) a rastergram display of $Ca^{2+}$ activity, where each dot represents the occurrence of a peak in the $Ca^{2+}$ response from each cell. (c) Representative images showing endothelial cells that were most sensitive (first 25% of endothelial cells to respond) to application of either ACh (green) or GSK (red). On average, 32.6% of cells that responded to one agonist also responded to the other (indicated by yellow in right most panel; $n$ = 3). Scale bars = 20 μm

The response to GSK was, initially, small localized $Ca^{2+}$ spikes which led to a slowly increasing global cytoplasmic $Ca^{2+}$ concentration (Figures 2b and S4). The GSK-evoked, global $Ca^{2+}$ elevation eventually plateaued, but the time taken to plateau was significantly longer when compared to ACh (Figure 1; 55.9 ± 6.4 s for GSK; 16.7 ± 4.7 s for ACh; $n$ = 6). Finally, large propagating $Ca^{2+}$ waves developed (Figure 2b,c and Movies S1 and S2). These waves propagated within and between cells at a constant velocity of ~5 to 15 $\mu m \cdot s^{-1}$ (Figure 2b,c, Movie S2, and Figure S5). GSK-evoked intracellular $Ca^{2+}$ waves were significantly lower in frequency than those for ACh (0.05 ± 0.01 Hz for GSK; 0.22 ± 0.03 Hz for ACh; $n$ = 6).

These results suggest there are at least major two components of the $Ca^{2+}$ signal arising from activation of TRPV4 channels: (a) initial local signals which lead to a slow global rise in $Ca^{2+}$ and (b) large fast propagating $Ca^{2+}$ waves.

We next sought to examine the mechanisms that give rise to the GSK-evoked $Ca^{2+}$ signals. We first confirmed the reproducibility of GSK-evoked responses (20 nM) in the same preparation so that a

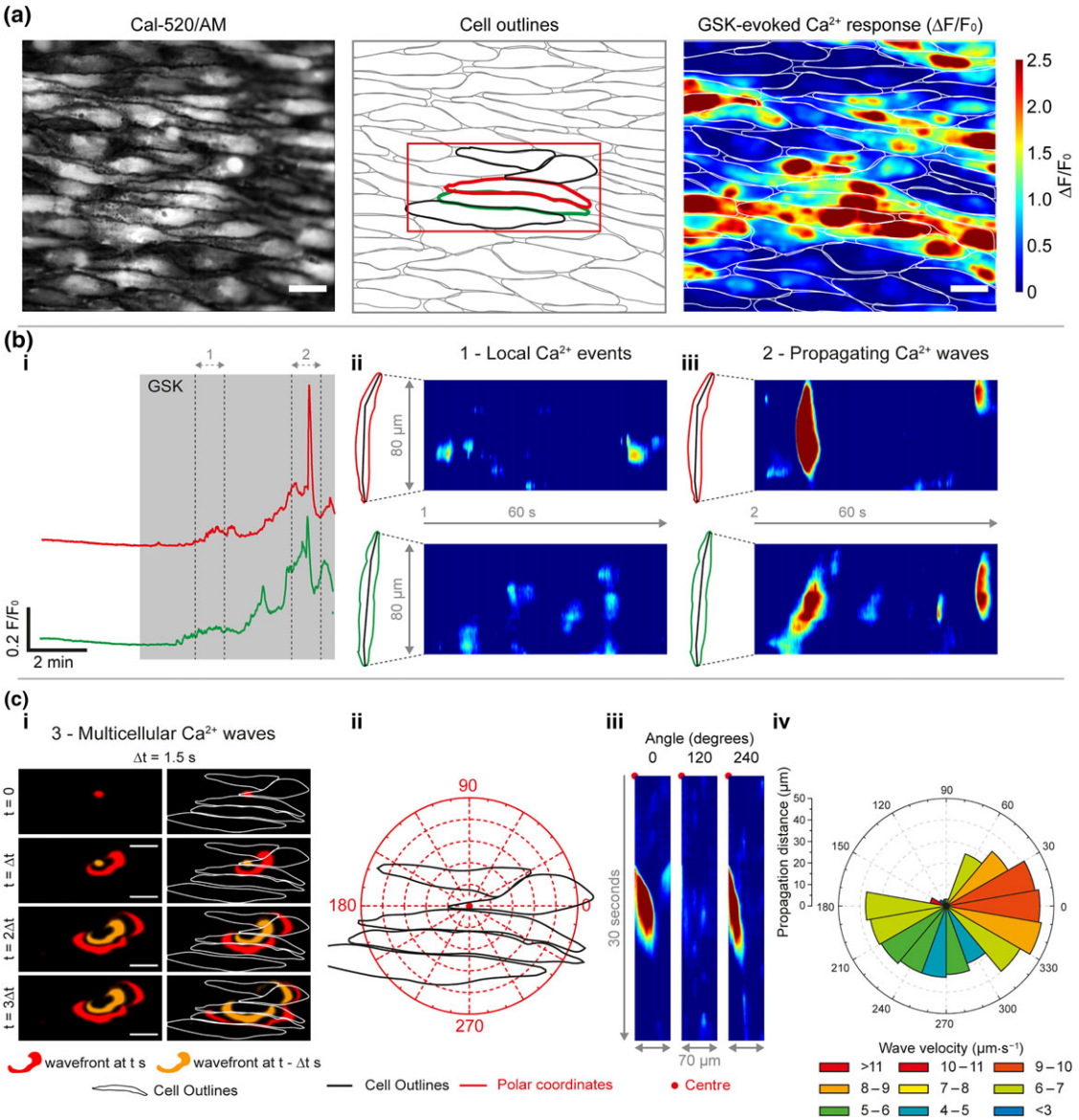


**FIGURE 2** Activation of TRPV4 channels stimulates local and propagating $Ca^{2+}$ events. (a) Representative $Ca^{2+}$ image (left), cell outlines (middle), and $\Delta F/F_0$ maximum intensity projection (right) illustrating the endothelial $Ca^{2+}$ response to activation of TRPV4 channels with GSK1016790A (GSK; 20 nM). The $\Delta F/F_0$ image shows an increase in $Ca^{2+}$ across the field of endothelial cells. (b) GSK stimulates local $Ca^{2+}$ events and propagating $Ca^{2+}$ waves. Panels show: (i) $Ca^{2+}$ traces illustrating the effect of GSK on whole-cell $Ca^{2+}$ levels from cells indicated by the coloured outlines in (a); (ii) line scans (kymographs) showing GSK-evoked local $Ca^{2+}$ events (1) and propagating $Ca^{2+}$ waves (2). Kymographs in (ii) correspond to the times indicated by dashed lines in (i) and were generated from $F/F_{\Delta t}$ movies, where $F_{\Delta t}$ is the running (20 s) baseline. (c) $Ca^{2+}$ waves propagate across multiple cells. Panels show: (i) time series of the active front (determined by sequential subtraction) of a multicellular $Ca^{2+}$ wave that spreads across four endothelial cells; (ii, iii) polar coordinate system (ii), example $F/F_{\Delta t}$ radial line scans (iii, 20° integration angle), and polar plot (iv) showing the angular dependence of propagation distance/velocity for the depicted $Ca^{2+}$ event. Data in (c) are shown in Movie S2. All scale bars = 20 μm

paired experimental design could be used to examine the effects of blockers. There was no significant difference in any of the $Ca^{2+}$ signal parameters measured (number of peaks, peak amplitudes, peak durations, 10–90% rise time, and 90–10% fall time) on repeated applications of GSK (Figure S3).

## 3.2 | $Ca^{2+}$ influx via TRPV4 channels is required to initiate endothelial $Ca^{2+}$signals

To examine the mechanisms underlying each component of the GSK-evoked $Ca^{2+}$ signal, we developed methods to extract the slow global rise in $Ca^{2+}$ and the propagating $Ca^{2+}$ waves (fast) component from raw $Ca^{2+}$ signals in each cell (Figure S1).

To determine if each component is dependent on $Ca^{2+}$ entry, we first performed experiments using a $Ca^{2+}$-free PSS (Figure 3a,b). The removal of extracellular $Ca^{2+}$ significantly decreased the percentage of cells exhibiting "slow" global $Ca^{2+}$ elevations and "fast" propagating waves in response to GSK (Figure 3c). The velocity of residual $Ca^{2+}$ waves was similar to those occurring in the presence of external $Ca^{2+}$ (Figure 3d; 10.0 ± 1.1 $\mu m \cdot s^{-1}$ for control; 8.8 ± 0.7 $\mu m \cdot s^{-1}$ for $Ca^{2+}$-free; $n$ = 5). However, removal of external $Ca^{2+}$ significantly reduced the amplitude (Figure 3e; 0.28 ± 0.11 $\Delta F/F_0$ for control; 0.02 ± 0.10 $\Delta F/F_0$ for $Ca^{2+}$-free; $n$ = 6) and the frequency of occurrence (Figure 3f; 4.1 ± 0.6 peaks per cell for control; 1.7 ± 0.1 peaks per cell for $Ca^{2+}$-free; $n$ = 6) of these residual propagating $Ca^{2+}$ waves.

These results suggest that $Ca^{2+}$ influx across the plasma membrane is essential for the slow global increase in $Ca^{2+}$ and for the propagating $Ca^{2+}$ waves evoked by GSK.

To test whether or not the slow global $Ca^{2+}$ rise and propagating $Ca^{2+}$ waves evoked by GSK arose from the activation of TRPV4 channels, we pre-incubated endothelial cells with the non-selective TRPV channel antagonist, **ruthenium red** (RuR; 5 μm, 20 min; Figure 4a,b). RuR significantly reduced the percentage of cells responding to GSK with slow global $Ca^{2+}$ elevations and propagating $Ca^{2+}$ waves (Figure 4c). Pretreatment with RuR reduced the amplitude (Figure 4e; 0.33 ± 0.06 $\Delta F/F_0$ for control; 0.07 ± 0.01 $\Delta F/F_0$ for RuR; $n$ = 6) and the frequency of occurrence (Figure 4f; 13.4 ± 3.3 peaks per cell for

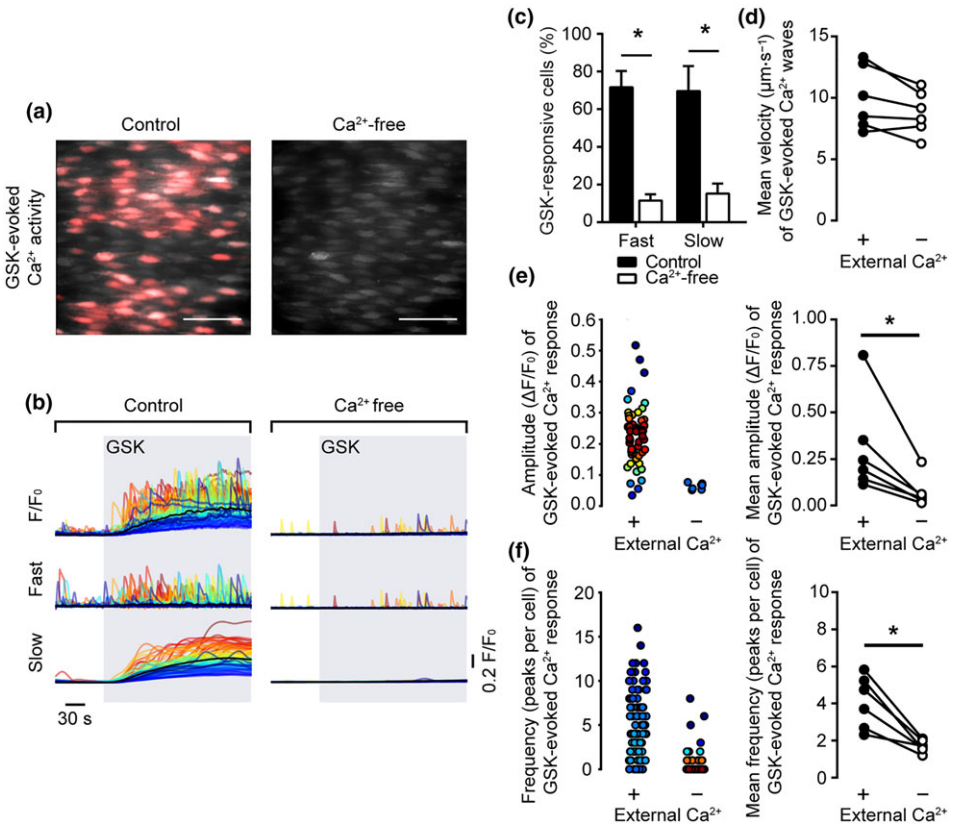


**FIGURE 3** The removal of extracellular $Ca^{2+}$ abolishes GSK-evoked $Ca^{2+}$ signalling. (a) Composite images showing GSK1016790A (GSK)-evoked $Ca^{2+}$ activity in a single field of native mesenteric artery endothelial cells before (left, control) and after (right, $Ca^{2+}$-free) the removal of external $Ca^{2+}$. Images show basal Cal-520/AM fluorescence (grey) with $Ca^{2+}$ activity overlaid (red). Scale bars = 50 μm. (b) GSK-evoked (20 nM; grey box) cellular $Ca^{2+}$ signals ($F/F_0$) in the presence (left) and absence (right) of extracellular $Ca^{2+}$. $F/F_0$ signals (top) were decomposed into fast (middle) and slow (bottom) components. (c) Summary bar chart showing the percentage of cells that exhibited propagating $Ca^{2+}$ waves (fast) and slow global $Ca^{2+}$ elevations (slow). (d–f) Paired summary data showing the effect of external $Ca^{2+}$ inhibition on $Ca^{2+}$ wave propagation velocity (d), peak amplitude ($\Delta F/F_0$, e), and the number of peaks per cell (f). The left plots in (e and f) are scatter plots showing the mean $Ca^{2+}$ event amplitude, or oscillation frequency, within each cell visualized in the experiment shown in panels (a and b). Individual data points are coloured (from blue, low to red, high) according to the density (i.e., occurrence) of particular values. *$P$ < .05, significantly different as indicated; paired Student's $t$ test ($n$ = 6)

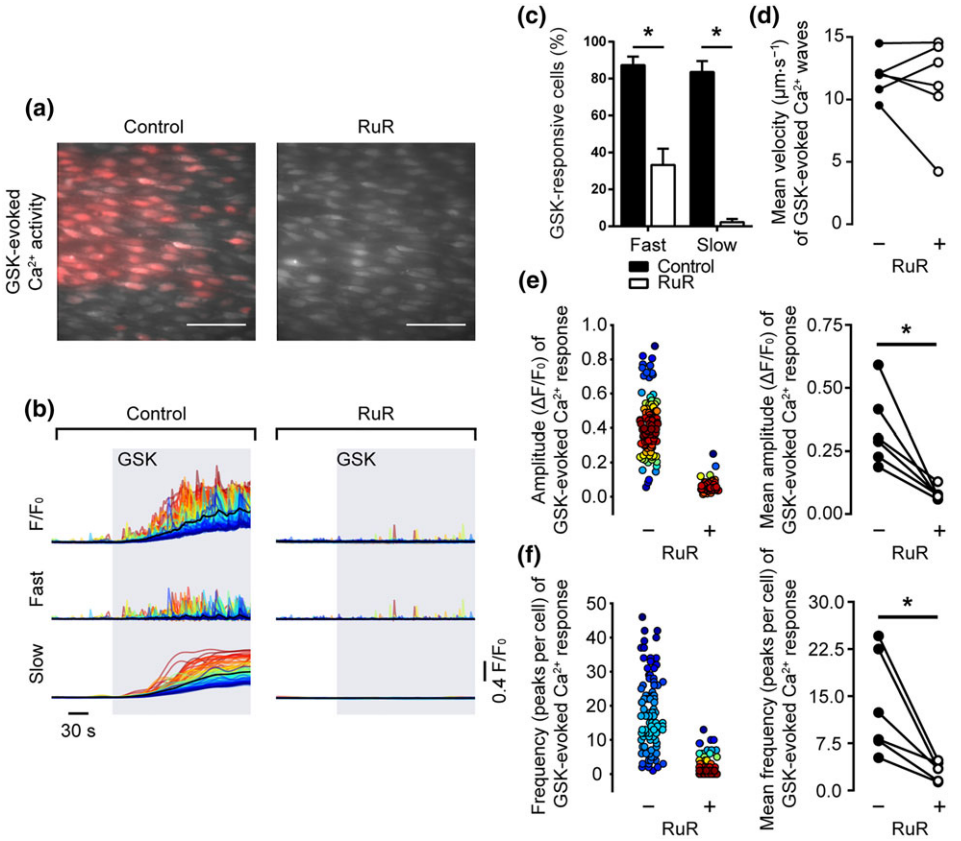


**FIGURE 4** Inhibition of TRPV channels with ruthenium red inhibits propagating $Ca^{2+}$ waves and slow global $Ca^{2+}$ elevations evoked by GSK1016790A. (a) Composite images showing GSK1016790A (GSK)-evoked (20 nM) $Ca^{2+}$ activity in the absence (left) and presence (right) of the broad-spectrum TRPV channel antagonist ruthenium red (RuR; 5 μM, 20 min) in the same native mesenteric artery endothelial cells. Images show basal Cal-520/AM fluorescence (grey) with $Ca^{2+}$ activity overlaid (red). Scale bars = 50 μm. (b) Raw $F/F_0$ (top), fast (middle), and slow (bottom) components of the GSK-evoked (20 nM; grey box) $Ca^{2+}$ signal in the absence (left) and presence (right) of RuR. (c) Summary bar chart illustrating the effect of RuR on the percentage of cells exhibiting propagating $Ca^{2+}$ waves and slow global $Ca^{2+}$ signal components. (d–f) Paired summary data showing the effect of TRPV channel inhibition on $Ca^{2+}$ wave propagation velocity (d), peak amplitude ($\Delta F/F_0$, e), and the number of peaks per cell (f). The left plots in (e–f) are scatter plots showing the mean $Ca^{2+}$ event amplitude, or oscillation frequency, within each cell visualized in the experiment shown in panels (a and b). Individual data points are coloured (from blue, low to red, high) according to the density (i.e., occurrence) of particular values. *$P < .05$, significantly different as indicated; paired Student's $t$ test ($n = 6$)

control; 3.2 ± 0.1 peaks per cell for RuR; $n = 6$) of propagating $Ca^{2+}$ waves but had no effect on the velocity of propagating waves (Figure 4d; 11.8 ± 0.7 μm·s$^{-1}$ for control; 11.6 ± 1.7 μm·s$^{-1}$ for RuR; $n = 5$). A similar reduction in GSK-evoked $Ca^{2+}$ signalling was observed using the selective TRPV4 channel antagonist, HC067047 (HC067; 10 μM, 20 min; Figure 5a,b). HC067 reduced the percentage of cells exhibiting slow, global elevations and the percentage exhibiting fast, propagating $Ca^{2+}$ waves (Figure 5c). HC067 reduced the amplitude (Figure 5e; 0.29 ± 0.08 $\Delta F/F_0$ for control; 0.08 ± 0.02 $\Delta F/F_0$ for HC067; $n = 6$) and the frequency (Figure 5f; 5.5 ± 0.8 peaks per cell for control; 0.7 ± 0.2 peaks per cell for HC067; $n = 6$) of propagating $Ca^{2+}$ waves. The velocity of residual $Ca^{2+}$ waves was unaffected by HC067 (Figure 5d; 13.1 ± 0.8 μm·s$^{-1}$ for control; 13.6 ± 0.7 μm·s$^{-1}$ for HC067; $n = 5$).

Together, these results suggest that $Ca^{2+}$ influx via TRPV4 channels is required to induce both the slow global rise component and the propagating $Ca^{2+}$ waves induced by GSK.

### 3.3 | GSK-induced $Ca^{2+}$waves require a replete internal $Ca^{2+}$ store, $IP_3$ synthesis, and $IP_3$ receptor activation

Having confirmed a role for TRPV4-mediated $Ca^{2+}$ influx in GSK-stimulated $Ca^{2+}$ signals, we next investigated the contribution of the internal $Ca^{2+}$ store using the sarcoplasmic/endoplasmic reticulum $Ca^{2+}$-ATPase (SERCA) inhibitor, CPA (Figure 6a,b). Depletion of the internal store by CPA decreased the percentage of cells exhibiting the slow global rise component of the GSK-evoked $Ca^{2+}$ signal and the percentage of cells in which propagating $Ca^{2+}$ waves occurred (Figure 6c). CPA significantly inhibited the wave propagation speed (Figure 6d; 8.6 ± 0.4 μm·s$^{-1}$ for control; 3.6 ± 0.5 μm·s$^{-1}$ for CPA; $n = 6$), amplitude (Figure 6e; 0.48 ± 0.12 $\Delta F/F_0$ for control; 0.17 ± 0.04 $\Delta F/F_0$ for CPA; $n = 6$), and frequency (Figure 6f; 4.3 ± 0.4 peaks per cell for control; 1.5 ± 0.2 peaks per cell for CPA; $n = 6$) of $Ca^{2+}$ waves. The amplitude of the slow global $Ca^{2+}$ rise

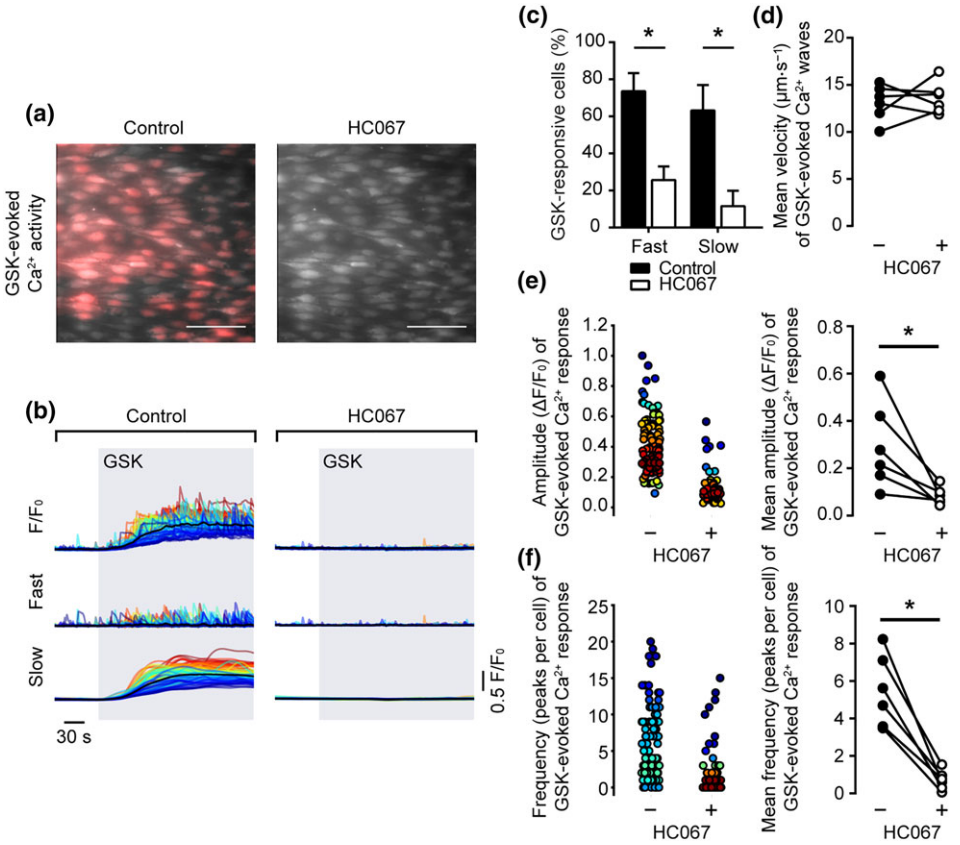


**FIGURE 5** Inhibition of TRPV4 channels with HC067047 inhibits both propagating $Ca^{2+}$ waves and slow global $Ca^{2+}$ elevations evoked by GSK1016790A. (a) Composite images showing GSK1016790A (GSK)-evoked (20 nM) $Ca^{2+}$ activity in the absence (left) and presence (right) of the broad-spectrum TRPV channel antagonist HC067047 (HC067; 10 μM, 20 min) in the same native mesenteric artery endothelial cells. Images show basal Cal-520/AM fluorescence (grey) with $Ca^{2+}$ activity overlaid (red). Scale bars = 50 μm. (b) Raw $F/F_0$ (top), fast (middle), and slow (bottom) components of the GSK-evoked (grey box) $Ca^{2+}$ signal in the absence (left) and presence (right) of HC067. (c) Summary bar chart illustrating the effect of HC067 on the percentage of cells exhibiting propagating $Ca^{2+}$ waves and slow global $Ca^{2+}$ signal components. (d–f) Paired summary data showing the effect of TRPV4 channel inhibition on $Ca^{2+}$ wave propagation velocity (d), peak amplitude ($\Delta F/F_0$, e), and the number of peaks per cell (f). The left plots in (e–f) are scatter plots showing the mean $Ca^{2+}$ event amplitude, or oscillation frequency, within each cell visualized in the experiment shown in panels (a and b). Individual data points are coloured (from blue, low to red, high) according to the density (i.e., occurrence) of particular values. *$P$ < .05, significantly different as indicated; paired Student's $t$ test ($n$ = 6)

initially appeared to be reduced by CPA (Figure 6b). However, this apparent decrease appears to occur in large part because of the increase in baseline $Ca^{2+}$ evoked by CPA and the non-linear relationship between $Ca^{2+}$ concentration and $F/F_0$ value. When the signals were calibrated (see Section 2), the mean $Ca^{2+}$ concentration increase evoked by GSK was 123 ± 75 nM, but after CPA, GSK evoked a $Ca^{2+}$ rise of 93 ± 44 nM ($n$ = 3), showing no significant effect of CPA. CPA itself evoked an increase in $Ca^{2+}$ concentration from a resting value of 176 ± 52 to 335 ± 58 nM ($n$ = 3). The elevated $Ca^{2+}$ may account for the reduced number of cells activated by GSK (Watanabe et al., 2003). These results suggest that the internal store is required for the propagating $Ca^{2+}$ waves.

To explore the role of $Ca^{2+}$ release from the internal store, we examined the contribution of $IP_3$ using pharmacological inhibition of phospholipase C (PLC; Figure 7a,b). The PLC inhibitor, U73122, significantly reduced the percentage of cells activated by GSK, both for the fast propagating $Ca^{2+}$ waves and for the slow persistent $Ca^{2+}$ elevation (Figure 7c). Although the mean amplitude of propagating $Ca^{2+}$ waves was not significantly different in the presence of U73122 (1.32 ± 0.25 $\Delta F/F_0$ for control; 0.67 ± 0.14 for U73122; $n$ = 5), there was a significant reduction in the propagation velocity (10.2 ± 0.4 μm·$s^{-1}$ for control; 5.5 ± 0.7 μm·$s^{-1}$ for U73122; $n$ = 5) and frequency of those events (Figure 7d-f).

U73343, the inactive analogue of the PLC inhibitor U73122, had no effect on GSK-induced $Ca^{2+}$ signals (Figure S6). The percentage of cells exhibiting slow and propagating $Ca^{2+}$ wave components of the GSK-evoked signal were unaltered. Pretreatment with U73343 did not significantly alter the propagation velocity (9.4 ± 0.4 μm·$s^{-1}$ for control; 7.7 ± 0.3 μm·$s^{-1}$ for U73343; $n$ = 5), amplitude (1.34 ± 0.26 $\Delta F/F_0$ for control; 1.34 ± 0.14 for U73343; $n$ = 5), nor the frequency (3.5 ± 0.3 peaks/cell for control; 4.3 ± 0.6 peaks/cell for U73343; $n$ = 5) of propagating $Ca^{2+}$ waves. Moreover, although

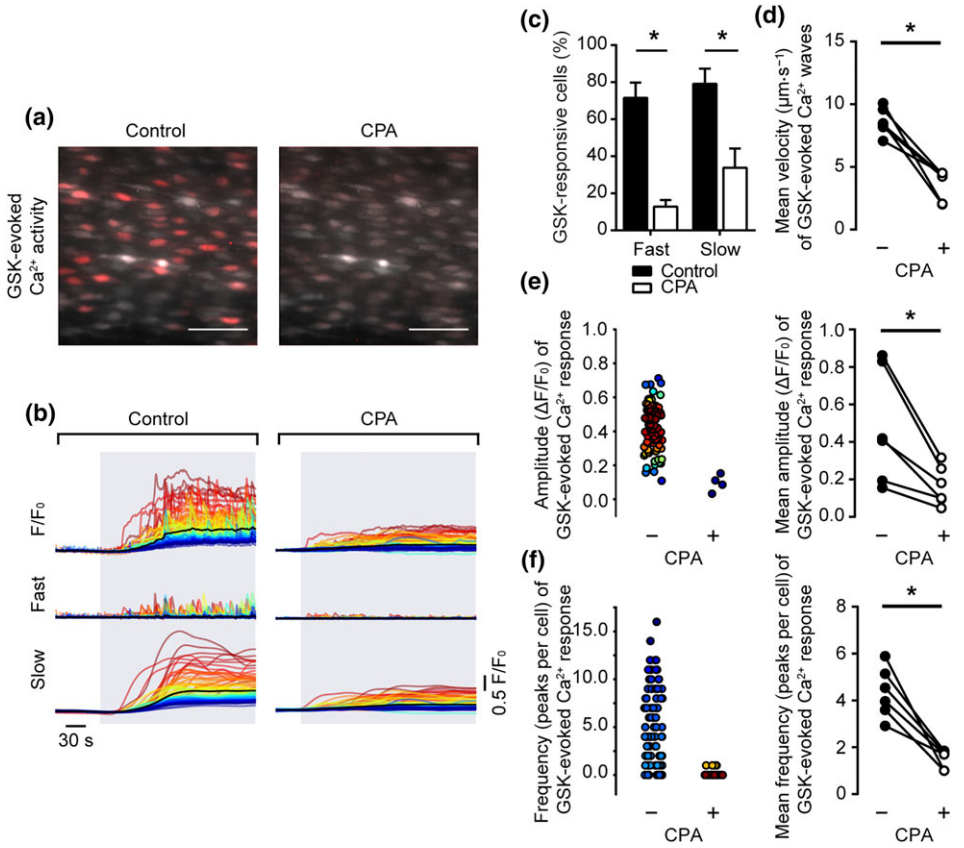


**FIGURE 6** Depletion of the internal $Ca^{2+}$ store modifies the $Ca^{2+}$ signal induced by activation of TRPV4 channels. (a) Composite images showing GSK1016709A (GSK)-evoked $Ca^{2+}$ activity in the absence (left) and presence (right) of cyclopiazonic acid (CPA; 10 μM, 5 min) in the same native mesenteric artery endothelial cells. Images show basal Cal-520/AM fluorescence (grey) with $Ca^{2+}$ activity overlaid (red). Scale bars = 50 μm. (b) GSK-evoked (20 nM; grey box) cellular $Ca^{2+}$ signals in the absence and presence of CPA (left and right respectively). Original $F/F_0$ traces (top) were decomposed into fast (middle) and slow (bottom) components. CPA evoked a substantial increase in basal $Ca^{2+}$ (see Section 3). In control and in the presence of CPA, $F/F_0$ was normalized to the $Ca^{2+}$ change before GSK so that the resting values in each case were 1. CPA caused a substantial increase in resting $Ca^{2+}$ (see text). (c) Summary bar chart illustrating the effect of CPA on the percentage of cells exhibiting propagating $Ca^{2+}$ waves and slow global $Ca^{2+}$ elevations to GSK. (d–f) Paired summary data showing the effect of SERCA inhibition on $Ca^{2+}$ wave propagation velocity (d), peak amplitude ($\Delta F/F_0$, e), and the number of peaks per cell (f). The left plots in (e–f) are scatter plots showing the mean $Ca^{2+}$ event amplitude, or oscillation frequency, within each cell visualized in the experiment shown in panels (a and b). Individual data points are coloured (from blue, low to red, high) according to the density (i.e., occurrence) of particular values. *$P < .05$, significantly different as indicated; paired Student's $t$ test ($n = 6$)

U73122 inhibits the internal store $Ca^{2+}$ pump in colonic smooth muscle cells (Macmillan & McCarron, 2010), the blocker did not reduce $IP_3$-evoked $Ca^{2+}$ release in endothelial cells (Figure S7).

These results suggest that the GSK-evoked slow global rise in $Ca^{2+}$ and propagating $Ca^{2+}$ waves each have contributions from PLC activation.

To investigate any role of $IP_3$-sensitive $Ca^{2+}$ stores in propagating $Ca^{2+}$ waves induced by activation of TRPV4 channels, we examined the effects of the $IP_3R$ antagonist, 2-APB, on GSK-evoked endothelial $Ca^{2+}$ signalling (Figure 8). 2-APB significantly reduced the percentage of cells exhibiting propagating $Ca^{2+}$ waves but had no effect on the percentage of cells exhibiting slow global elevations in $Ca^{2+}$ in response to GSK (Figure 8c). 2-APB had no effect on the amplitude (0.67 ± 0.09 $\Delta F/F_0$ for control; 0.60 ± 0.15 $\Delta F/F_0$ for 2-APB; $n = 6$) but significantly reduced propagation velocity (11.0 ± 0.8 $\mu m \cdot s^{-1}$ for control; 2.0 ± 0.4 $\mu m \cdot s^{-1}$ for 2-APB; $n = 5$) and frequency (3.1 ± 0.3 peaks per cell for control; 0.9 ± 0.3 peaks per cell for 2-APB; $n = 6$) of fast $Ca^{2+}$ waves (Figure 8d–f).

To crosscheck the contribution of $IP_3Rs$ in the propagating $Ca^{2+}$ waves, we used caffeine—a potent inhibitor of $IP_3Rs$ (Ehrlich, Kaftan, Bezprozvannaya, & Bezprozvanny, 1994; Parker & Ivorra, 1991; Saleem, Tovey, Molinski, & Taylor, 2014). Caffeine, which does not evoke $Ca^{2+}$ release in the endothelial cells under study and inhibits $Ca^{2+}$ release evoked by $IP_3$ (Wilson et al., 2019), also blocked GSK-evoked propagating $Ca^{2+}$ waves (Figure S8). Interestingly, caffeine also reduced the slow global $Ca^{2+}$ rise suggesting an effect of caffeine also on TRPV4 channels.

While $Ca^{2+}$ influx via TRPV4 channels triggered large propagating $Ca^{2+}$ waves from the internal $Ca^{2+}$ store, the release and influx did not become an uncontrolled self-regenerative process but remained under the control of $Ca^{2+}$ influx. When activation of TRPV4 channels ceases, by washout of GSK, the propagating $Ca^{2+}$ waves stop (Figure S9 and Movie S3), and $Ca^{2+}$ returned towards resting values.

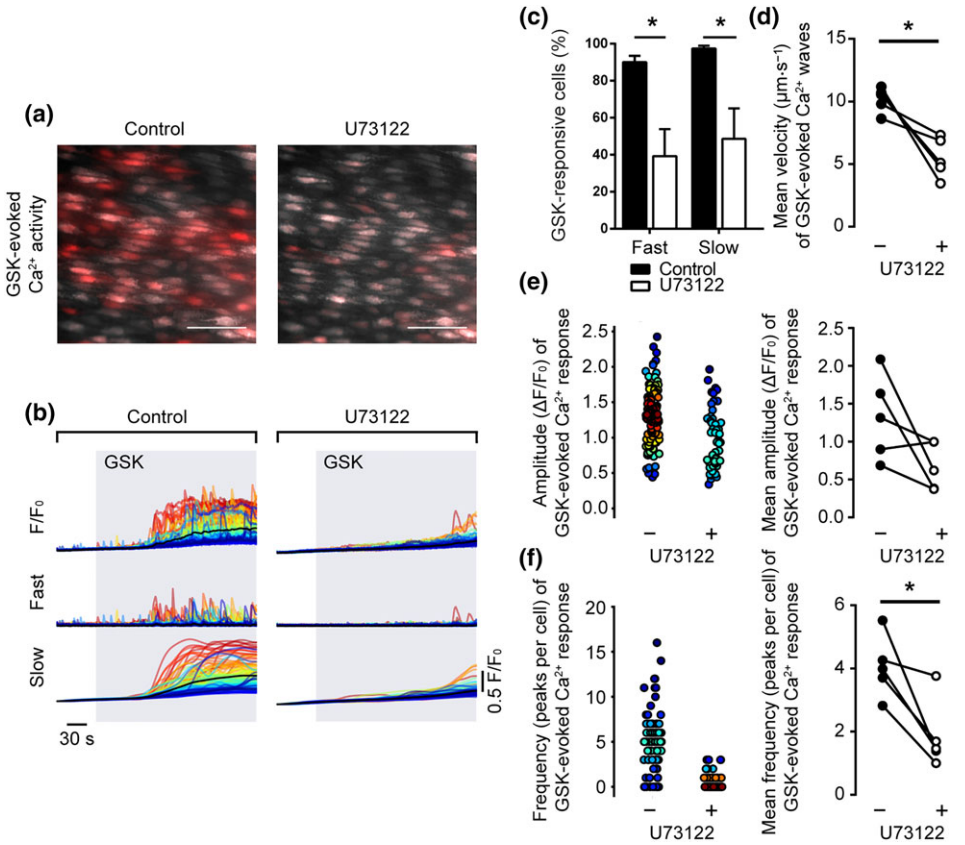


**FIGURE 7** PLC inhibition reduces the slow global $Ca^{2+}$ rises and propagating $Ca^{2+}$ waves of the GSK-evoked $Ca^{2+}$ response. (a) Composite images illustrating GSK1016790A (GSK)-evoked (20 nM) $Ca^{2+}$ activity in the absence (left) and presence (right) of the PLC antagonist U73122 (2 μM, 10 min) in a single field of native mesenteric artery endothelial cells. Images show basal Cal-520/AM fluorescence (grey) with $Ca^{2+}$ activity overlaid (red). Scale bars = 50 μm. (b) GSK-evoked $F/F_0$ (top) $Ca^{2+}$ signals, and corresponding fast (middle) and slow (bottom) signal components in the absence (left) and presence (right) of U73122. (c) Summary data showing the effect of U73122 on the percentage of endothelial cells exhibiting propagating $Ca^{2+}$ waves (fast) and global $Ca^{2+}$ elevations (slow). (d–f) Paired summary data showing the effect of PLC inhibition on $Ca^{2+}$ wave propagation velocity (d), peak amplitude ($\Delta F/F_0$, e), and the number of peaks per cell (f). The left plots in (e–f) are scatter plots showing the mean $Ca^{2+}$ event amplitude, or oscillation frequency, within each cell visualized in the experiment shown in panels (a and b). Individual data points are coloured (from blue, low to red, high) according to the density (i.e., occurrence) of particular values. *$P < .05$, significantly different as indicated; paired Student's *t* test ($n = 5$)

This result demonstrates that TRPV4 channels maintain control of $Ca^{2+}$ release from the internal $Ca^{2+}$ store and the propagation of $Ca^{2+}$ waves both within and between cells.

## 3.4 | The functional effects of TRPV4 channels in controlling vascular tone

Collectively, our results suggest that endothelial TRPV4-mediated $Ca^{2+}$ influx activates $Ca^{2+}$-induced $Ca^{2+}$ release at $IP_3Rs$. To investigate any physiological contribution of this process, we examined vascular tone in mesenteric arteries (Figure 8) with and without a functionally intact endothelial layer.

In intact, pressurized arteries, ACh and GSK each relaxed arteries and reversed phenylephrine-mediated contractions (Figure S10; $n = 5$). Relaxations to GSK were reversed by the selective TRPV4 channel antagonist, HC067. However, the dilations to ACh were preserved after blockade of TRPV4 channels with HC067 (Figure S10; $n = 5$). These results suggest that these channels do not contribute to ACh-evoked relaxations in rat mesenteric arteries (see also Hartmannsgruber et al., 2007; Kohler et al., 2006; Wilson, Lee, & McCarron, 2016).

We next investigated the contribution of the internal $Ca^{2+}$ store to TRPV4-mediated relaxation evoked by GSK. In *en face* preparations (225 ± 4 μm resting diameter; $n = 10$), ACh and GSK each relaxed phenylephrine-constricted arteries back to pre-constricted levels (Figure 9 and Figure S2). In these same arteries, the removal of the endothelium increased the sensitivity to phenylephrine and significantly reduced relaxation to ACh (to 26 ± 7%; $n = 5$ vs. control with endothelium). The residual ACh-evoked response may have arisen from the incomplete removal of the endothelium. The functional removal of the endothelium also prevented GSK-evoked relaxations. Indeed, after the removal of the endothelium, GSK caused an increase in tone (Figure 9e; $n = 5$). Endothelium removal did not prevent relaxation to the endothelium-independent vasodilator SNP (Figure 9).

These results demonstrate that vascular relaxation to GSK occurs via an endothelium-dependent mechanism and not by acting directly on the underlying smooth muscle.

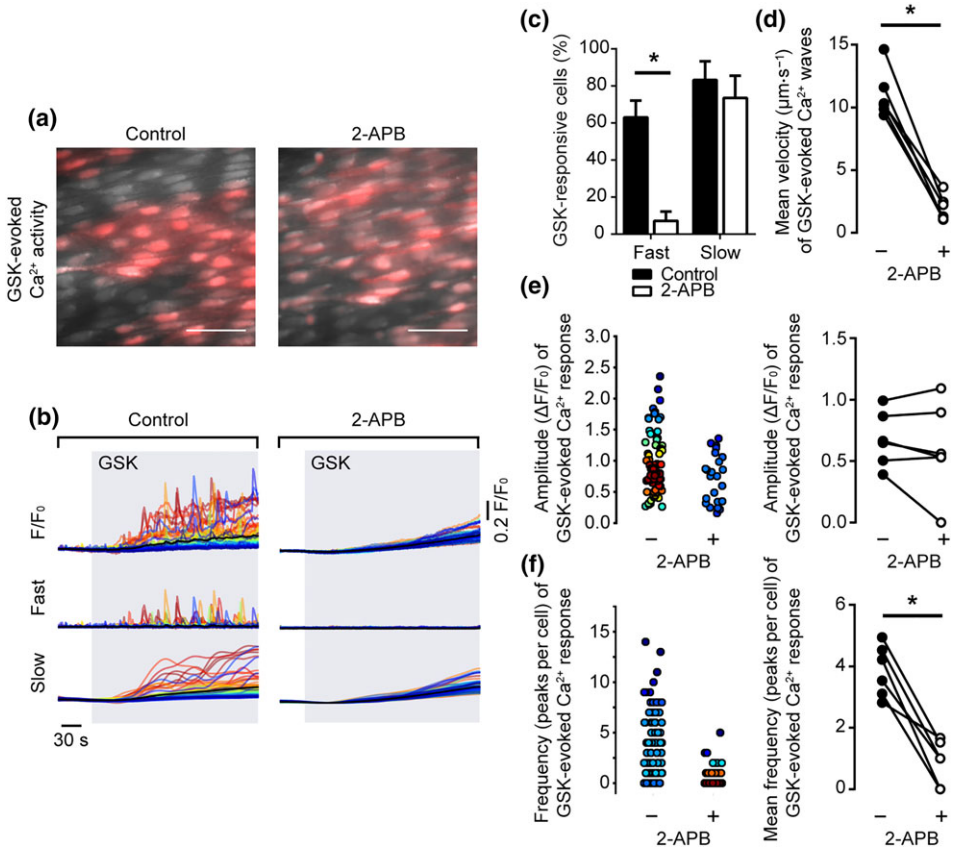


**FIGURE 8** Inhibiting $IP_3$ receptors prevents propagating $Ca^{2+}$ waves but not slow global $Ca^{2+}$ elevations induced by activation of TRPV4 channels. (a) Composite images showing $Ca^{2+}$ activity evoked by GSK1016790A (GSK, 20 nM) in the absence (left) and presence (right) of the $IP_3R$ antagonist, 2-APB (500 μM, 10 min) in a single field of native mesenteric artery endothelial cells. Images show basal Cal-520/AM fluorescence (grey) with $Ca^{2+}$ activity overlaid (red). Scale bars = 50 μm. (b) GSK-evoked (grey box) cellular $Ca^{2+}$ signals ($F/F_0$; top) were decomposed into fast (middle) and slow (bottom) components. (c) Summary data illustrating the percentage of cells exhibiting propagating $Ca^{2+}$ waves and slow global $Ca^{2+}$ increases. (d–f) Paired summary data showing the effect of $IP_3R$ inhibition on $Ca^{2+}$ wave propagation velocity (d), peak amplitude ($\Delta F/F_0$, e), and the number of peaks per cell (f). The left plots in (e–f) are scatter plots showing the mean $Ca^{2+}$ event amplitude, or oscillation frequency, within each cell visualized in the experiment shown in panels (a and b). Individual data points are coloured (from blue, low to red, high) according to the density (i.e., occurrence) of particular values. *$P < .05$, significantly different as indicated; paired Student's $t$ test ($n = 6$)

### 3.5 | Store dependence of the TRPV4 channel response

We next examined the contribution of $Ca^{2+}$-induced $Ca^{2+}$ release at $IP_3Rs$ in TRVP4 mediated relaxation. To do this, we assessed the effect of GSK on vascular reactivity before and after depletion of internal $Ca^{2+}$ stores.

Depletion of the internal $Ca^{2+}$ store using CPA (6 μM) prevents stable contractions such that it was not possible to reliably assess vasodilator responses in these arteries. Instead, we examined whether pretreatment with GSK was capable of modulating PE-evoked contraction (Figure 10). Pretreatment with GSK significantly attenuated PE-induced contractions (Figure 10a, c).

After $Ca^{2+}$ store depletion using CPA, a higher concentration of phenylephrine (3.6 ± 0.2 μM for control; 12.8 ± 2.2 μM for CPA; $n = 5$) was required to achieve a level of contraction (20 ± 2%; $n = 5$) equivalent to control conditions (Figure S2). After store depletion with CPA, pretreatment with GSK no longer attenuated phenylephrine-induced contraction (4 ± 2% contraction for GSK; 27 ± 6% contraction for GSK + CPA; $n = 5$; $P < .05$). Rather, GSK tended to enhance the contraction to phenylephrine (Figure 10b, c). Together, these results demonstrate that depletion of internal $Ca^{2+}$ stores reduces the inhibitory effect of GSK pretreatment on phenylephrine-induced contraction.

## 4 | DISCUSSION

TRPV4 channels are emerging as key plasmalemmal channels that mediates $Ca^{2+}$ influx and physiological functions in the endothelium (Fiorio Pla et al., 2012; Gao & Wang, 2010; Gifford et al., 2014; Ma et al., 2013; Sayed et al., 2010; Schierling et al., 2011; Sonkusare et al., 2012; Thodeti et al., 2009; Troidl et al., 2009). We have shown that the $Ca^{2+}$ increase in endothelial cells, arising from $Ca^{2+}$ entry via TRPV4 channels, may be amplified by a $Ca^{2+}$-induced $Ca^{2+}$ release-like

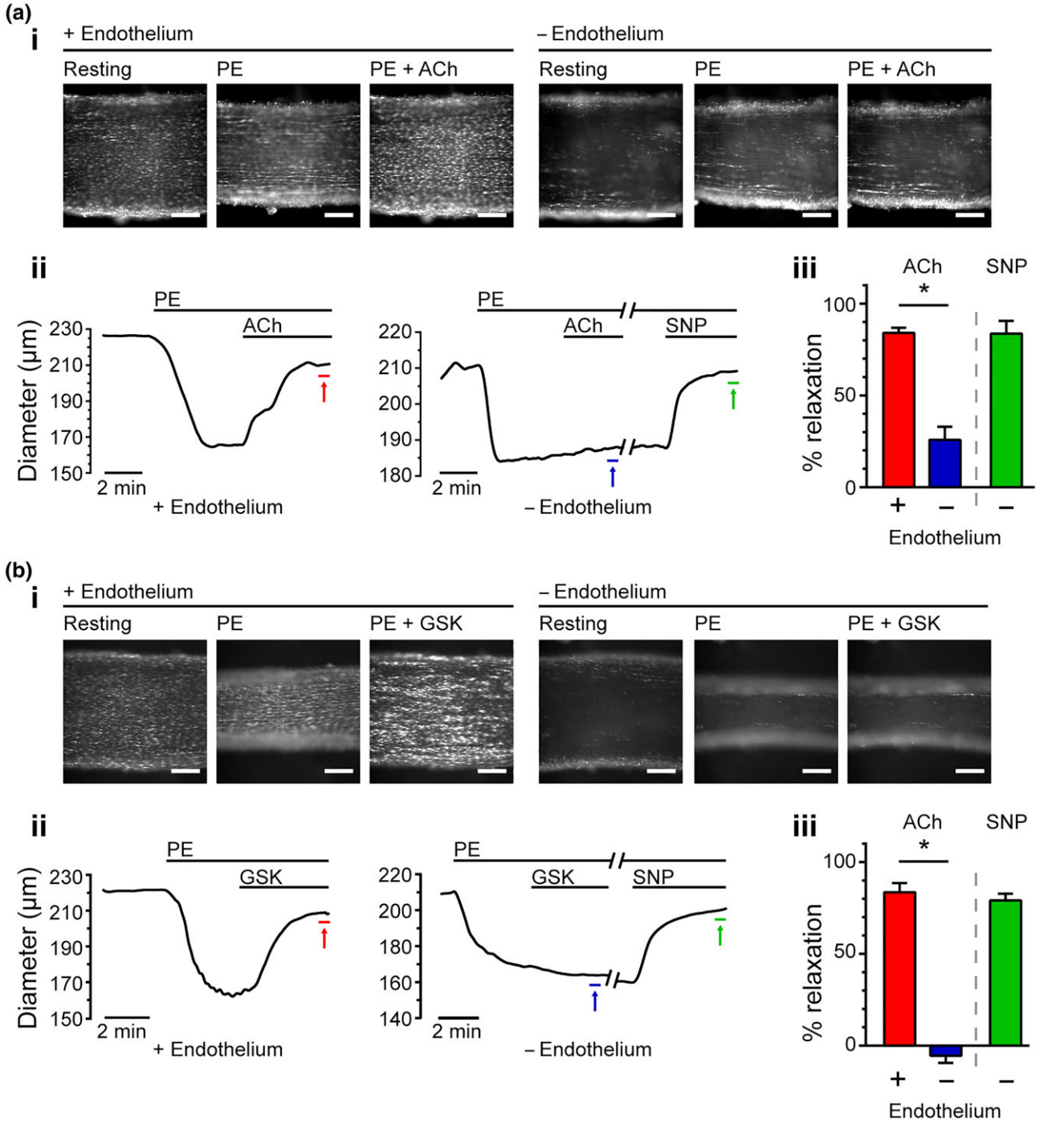


**FIGURE 9** ACh and GSK1016790A both cause endothelium-dependent vasodilation. (a and b) The vasodilator effect of ACh (a; 100 nM) and GSK1016790A (b; GSK; 20 nM) on phenylephrine (PE)-contracted arteries before (+ endothelium) and after the mechanical removal of the endothelium (– endothelium). After the removal of the endothelium, sodium nitroprusside (SNP) was used to test endothelium-independent vasodilation. Panels show: (i) images of an *en face* artery, illustrating the vessel's responses to phenylephrine and either ACh or GSK (in the continued presence of phenylephrine ); (ii) full time course of the experiments shown in the corresponding panel (i); (iii) Summary data (mean ± SEM, $n = 5$) illustrating the effect of the endothelium removal on vasodilator responses to the indicated agonist. Relaxations are expressed as % change from PE-induced tone. A negative value indicates an enhancement of phenylephrine-induced contraction. Coloured arrows in (ii) indicate the time at which relaxation to each agonist was assessed. All scale bars = 100 μm. $^*P < .05$, significantly different as indicated; repeated measures one-way ANOVA with multiple comparison

mechanism acting at $IP_3Rs$ to generate propagating $Ca^{2+}$ waves. When $IP_3R$-mediated $Ca^{2+}$ release was inhibited, TRPV4-induced increases in intracellular [$Ca^{2+}$] and TRPV4-mediated control of vascular tone was supressed. These results highlight the significance of endothelial TRPV4-mediated $Ca^{2+}$-induced $Ca^{2+}$ release at $IP_3Rs$ in controlling vascular contractility (Figure 11).

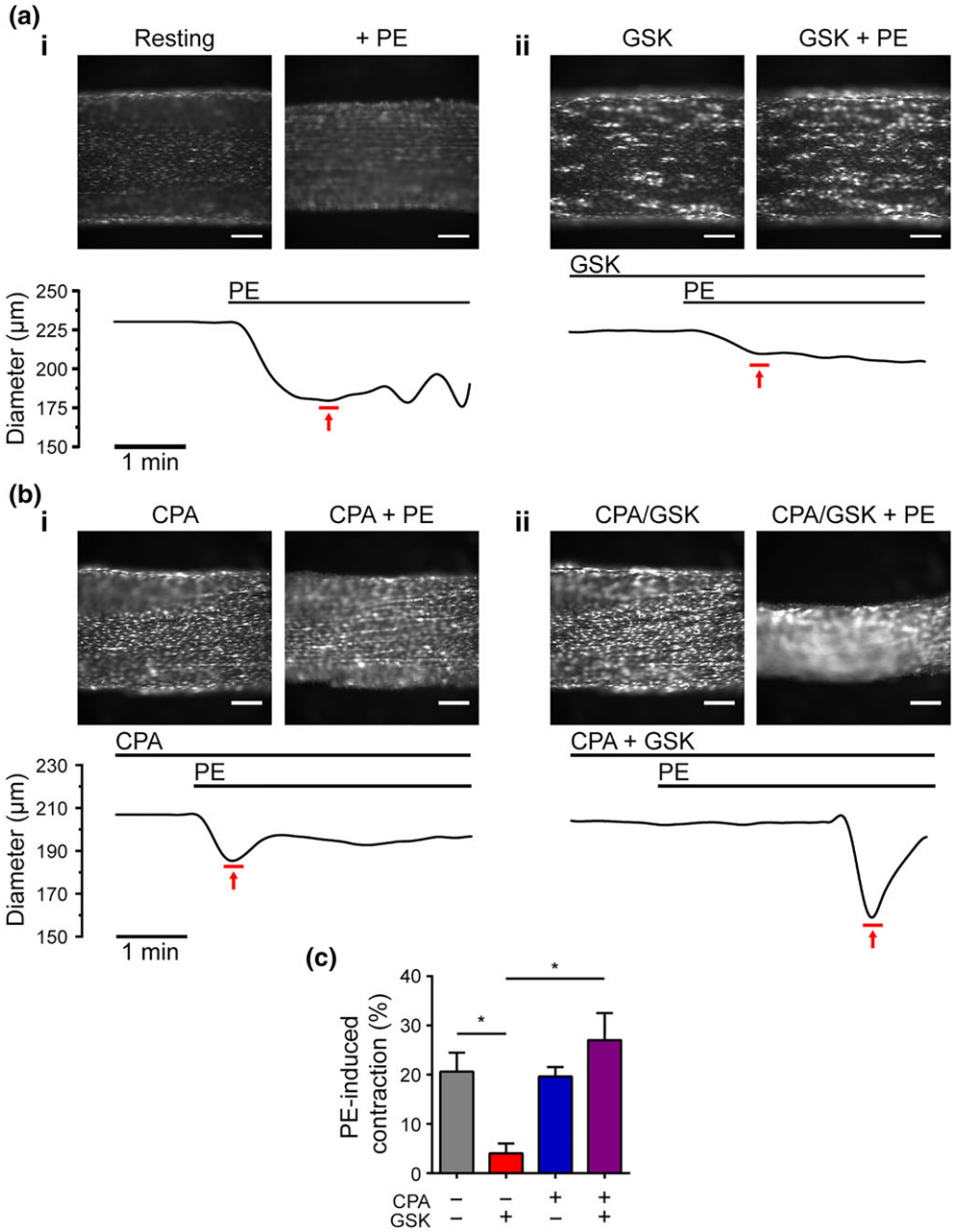


**FIGURE 10** $Ca^{2+}$ store depletion prevents TRPV4-mediated opposition of vascular tone. (a and b) Effect of GSK1016790A (GSK, 20 nM) on phenylephrine (PE)-induced contraction in vessels with an intact internal $Ca^{2+}$ store (a) or after depletion of the internal $Ca^{2+}$ store (b) using cyclopiazonic acid (CPA; 6 µm; bottom trace). Upper panels show images of *en face* arteries, pretreated with the indicated drug, before and after exposure to phenylephrine. Corresponding diameter traces are shown in the lower panels. Data in (i) and (ii) show responses from the same artery. Pretreatment with CPA and GSK consistently delayed the onset but increased the magnitude of the response to phenylephrine. The reason for the delay is not clear. All scale bars = 100 µm. (c) Summary data (mean ± SEM, $n$ = 5) showing the magnitude of phenylephrine-induced contraction (% resting diameter) under each of the conditions. Diameter measured at the times indicated by the red arrows on diameter traces. *$P$ < .05, significantly different as indicated; repeated measures one-way ANOVA with multiple comparisons

In this study, we analysed individual TRPV4-mediated $Ca^{2+}$ responses in large numbers of endothelial cells in intact blood vessels. Two components, a slow global increase and propagating $Ca^{2+}$ waves, contributed to the $Ca^{2+}$ response to activation of TRPV4 channels. The response to activation of TRPV4 channels was also heterogeneous among cells. Some cells were highly responsive, while other cells responded weakly or not at all (see also Aird, 2012; Huang, Chu, Chen, & Jen, 2000; Lee et al., 2018; Marie & Beny, 2002; McCarron, Lee, & Wilson, 2017; McCarron et al., 2019; Wilson, et al., 2016). We developed methods to automatically extract and separate the slow global increases and propagating $Ca^{2+}$ waves occurring in each endothelial cell. The changes in $Ca^{2+}$ concentration triggered by activation of TRPV4 channels consisted of different phases which operated sequentially. First, rapid localized $Ca^{2+}$ changes occurred

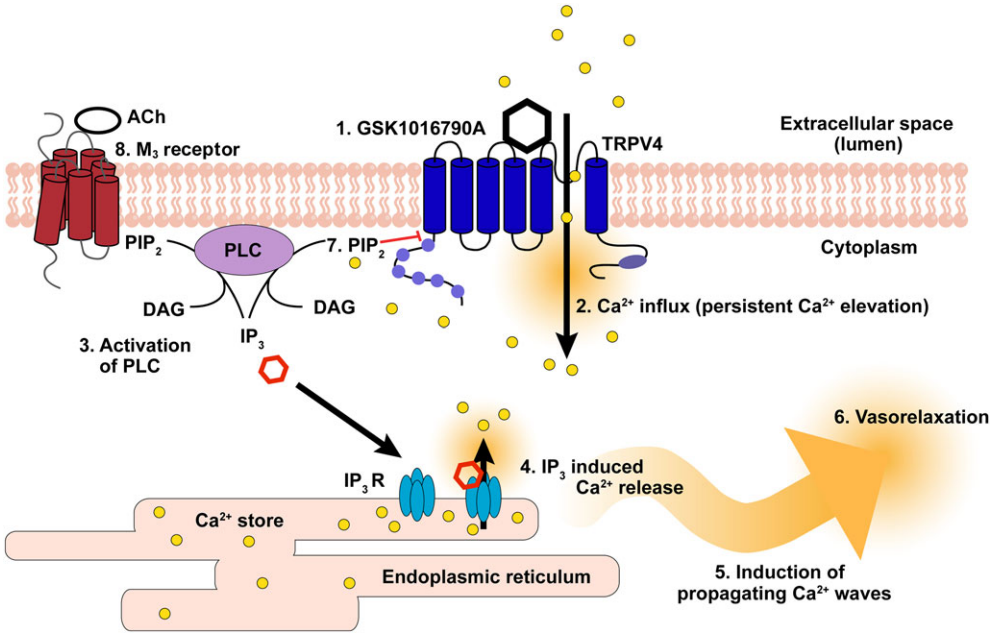


**FIGURE 11** Model of TRPV4-mediated control of vascular tone. Activation of TRPV4 channels (1) induces $Ca^{2+}$ influx which results in a persistent elevation in cytoplasmic $Ca^{2+}$ concentration (2). Basal (Hardie, Gu, Martin, Sweeney, & Raghu, 2004; Running Deer, Hurley, & Yarfitz, 1995; Willars, Nahorski, & Challiss, 1998) or $Ca^{2+}$-activated PLC (γ, δ, or β) activity decreases $PIP_2$ and generates $IP_3$ (3). $Ca^{2+}$ derived from TRPV4 channel activity together with $IP_3$ (McCarron, Chalmers, MacMillan, & Olson, 2010) act at $IP_3$ receptors on the internal $Ca^{2+}$ store to induce $Ca^{2+}$ release (4). The released $Ca^{2+}$ triggers propagating $Ca^{2+}$ waves (5) by activating neighbouring $IP_3$ receptors that ultimately result in vasodilation (6). The entire process remains under the control of $Ca^{2+}$ influx and terminates when TRPV4 channel activity ceases. This channel activity is suppressed by $PIP_2$ (7). ACh, via the **M3 receptor**, also activates PLC to generate $IP_3$ and activate $Ca^{2+}$ release from the store. The characteristics of $M_3$- and TRPV4-mediated $Ca^{2+}$ release differ significantly (see text)

which led to a slow persistent global elevation in $Ca^{2+}$ throughout the cytoplasm. Then, large transient increases as a result of propagating $Ca^{2+}$ waves occurred. The large transient increases as a result of propagating $Ca^{2+}$ waves dominated the $Ca^{2+}$ changes occurring in the endothelium after a short time (~30 s).

Each of the $Ca^{2+}$ changes occurring as a result of activation of TRPV4 channels was critically dependent on $Ca^{2+}$ influx across the plasma membrane. The $Ca^{2+}$ changes were abolished after the removal of external $Ca^{2+}$ or by the inhibition of TRPV4 channels, with RuR or HC067047. These results suggest that $Ca^{2+}$ influx via TRPV4 channels generates the persistent global $Ca^{2+}$ rise. Inhibiting $IP_3$-mediated $Ca^{2+}$ release by depleting the internal $Ca^{2+}$ store, or inhibiting $IP_3$Rs, had little effect on the slow persistent global elevation in $Ca^{2+}$ but prevented the large transient increases arising from propagating $Ca^{2+}$ waves. This result suggests that $Ca^{2+}$ entry via TRPV4 channels triggers activation of $IP_3$Rs which amplifies the initial $Ca^{2+}$ rise and initiates regenerative release of $Ca^{2+}$ in the form of propagating waves. In support of the active nature of the $Ca^{2+}$ waves, the velocity of wave progression away from the release site was relatively constant within and between cells (~5 to 15 $\mu m \cdot s^{-1}$). If diffusion alone was responsible for wave progression, velocity and amplitude would decline with distance from the release site. The mechanisms contributing to TRPV4-mediated activation of $Ca^{2+}$ release and propagation may include direct activation of $IP_3$Rs (in a $Ca^{2+}$-induced $Ca^{2+}$ release like process) or indirect $Ca^{2+}$-dependent activation of PLC. The partial inhibition of the propagating $Ca^{2+}$ waves by the PLC-blocker, U73122, is consistent with being a $Ca^{2+}$-induced $Ca^{2+}$ release-like process at $IP_3$Rs. Basal PLC activity has been reported for many PLC isoforms in biochemical experiments (Running Deer et al., 1995; Willars et al., 1998) and in living cells (Hardie et al., 2004; Willars et al., 1998) which may create a background level of $IP_3$ for $Ca^{2+}$-induced $Ca^{2+}$ release to occur.

Interestingly, blocking of PLC by U73122 also reduced the slow global $Ca^{2+}$ response (i.e., TRPV4-mediated $Ca^{2+}$ influx). Previous work has shown that TRPV4 channels are inhibited by the phospholipid, **phosphatidylinositol 4,5-bisphosphate** ($PIP_2$; Harraz, Longden, Hill-Eubanks, & Nelson, 2018). PLC-mediated depletion of $PIP_2$ results in disinhibition of TRPV4 channels and increased $Ca^{2+}$ influx (Harraz et al., 2018). Thus, blocking of PLC by U73122 might be expected to decrease TRPV4 channel activity.

To block $IP_3$Rs, we used both 2-APB and caffeine. 2-APB is a broad-spectrum inhibitor that, although effective in blocking $IP_3$Rs in native endothelial cells, may inhibit $Ca^{2+}$ entry pathways (see Peppiatt et al., 2003; Trebak, Bird, McKay, & Putney, 2002; Voets et al., 2001; Wilson, Lee, & McCarron, 2016). However, in the present experimental conditions, 2-APB did not reduce the slow global $Ca^{2+}$ rise evoked by activation of TRPV4 channels suggesting that it is not inhibiting influx in the present experiments. Caffeine, while often used as a RyR activator, is a potent inhibitor of $IP_3$Rs in the same concentration range used to activate RyR (Ehrlich et al., 1994; Parker & Ivorra, 1991; Saleem et al., 2014). Caffeine does not evoke $Ca^{2+}$ release in endothelial cells (Wilson, Saunter, Girkin, & McCarron, 2015) and inhibits $Ca^{2+}$ release induced by photolysis of caged-$IP_3$ in the endothelium (Wilson et al., 2019). That caffeine was effective in inhibiting propagating $Ca^{2+}$

waves supports the conclusion that $IP_3Rs$ contribute to TRPV4-mediated $Ca^{2+}$ responses.

RuR and HC067047 were each used to block TRPV4 channels. RuR is an effective TRPV4 channel antagonist but also has effects unrelated to this channnel. For example, RuR is an antagonist of channels such as the mitochondrial uniporter, the RyR, voltage-dependent $Ca^{2+}$ channels, and other TRP channels. However, the effects of RuR on these other channels are unlikely to explain the present findings. RuR is not membrane permeant and will not have access to the cytoplasm, so the effects on the mitochondrial uniporter or RyR are unlikely to be of significance in the present study. While RuR may have effects on voltage-sensitive $Ca^{2+}$ channels (Cibulsky & Sather, 1999), these channels do not appear to play a major role in endothelial $Ca^{2+}$ signalling. RuR may also inhibit other **TRP channels**, for example, TRPC and TRPA. However, those channels are not activated by the agonist used in the present study—GSK1016790A—suggesting that channels other than TRPV4 are unlikely contributors. The present findings with RuR are also supported by the use of the more selective TRPV4 channel antagonist HC067047 which also blocked the response to GSK1016790A. Together, the findings point to TRPV4 channels as being the major target for RuR in the present study.

The increase in cytoplasmic $Ca^{2+}$ concentration evoked by TRPV4-mediated $Ca^{2+}$-induced $Ca^{2+}$ release at $IP_3Rs$ is large and regenerative, as demonstrated by the long distance propagation. This process arises (at least in part) because $IP_3Rs$ are activated by $Ca^{2+}$. TRPV4 channels are also activated by $Ca^{2+}$ (Strotmann, Schultz, & Plant, 2003). The $Ca^{2+}$-dependent processes operating at $IP_3Rs$ and TRPV4 channels are positive feedback mechanisms that should self-reinforce and reach a maximum in all-or-none fashion. However, TRPV4-mediated $Ca^{2+}$-induced $Ca^{2+}$ release at $IP_3Rs$ does not become uncontrolled and, while regenerative, remains tightly regulated by $Ca^{2+}$ influx. The question arises as to why maximum responses do not occur each time TRPV4-mediated influx begins. The answer may lie in $IP_3Rs$ and TRPV4 channels being regulated to prevent uncontrolled influx and release (Foskett, White, Cheung, & Mak, 2007; Nilius, Watanabe, & Vriens, 2003). Two observations support this conclusion. First, when TRPV4-mediated $Ca^{2+}$ influx ceases, the release of $Ca^{2+}$ from $IP_3Rs$ stops. Thus, $Ca^{2+}$ release is tightly coupled to influx. Second, coordinated activity of $IP_3Rs$ is required for propagating waves to occur. The propagation of $Ca^{2+}$ waves requires sequential opening and then closing of $IP_3Rs$. Thus, after activation, the $IP_3R$ must become refractory to ensure a directional propagation of the signal. The decline in $Ca^{2+}$ occurring at the back of the wave presumably follows from a functional compartmentalization of the endoplasmic reticulum which renders the site of $IP_3$-mediated $Ca^{2+}$ release refractory to the phosphoinositide. The functional compartmentalization may arise from a lowered local $Ca^{2+}$ concentration in the lumen of the endoplasmic reticulum, or increased $Ca^{2+}$ concentrations could deactivate the receptors (Adkins & Taylor, 1999; McCarron, MacMillan, Bradley, Chalmers, & Muir, 2004; Oancea & Meyer, 1996). These observations highlight a system that is activated by $Ca^{2+}$ influx, but is regulated to prevent an uncontrolled positive feedback processes dominating the TRPV4-mediated increases in cytoplasmic $Ca^{2+}$ concentrations.

As well as propagating at a constant velocity within cells, TRPV4-mediated $Ca^{2+}$ waves could move seamlessly, at the same velocity, across cell boundaries into neighbouring cells as intercellular $Ca^{2+}$ waves (Movie S2). These waves were abolished by $IP_3R$ blockers or removal of GSK. The mechanisms of intercellular wave propagation are not entirely clear, but $IP_3Rs$ and (since the process stops when GSK is removed) TRPV4 channel activities are both required for these intercellular waves to occur.

In other tissues, intercellular $Ca^{2+}$ waves may be a fundamental mechanism for coordinating multicellular responses (Leybaert & Sanderson, 2012). In the endothelium of small arteries of the mouse cremaster muscle, rapidly spreading intercellular $Ca^{2+}$ waves propagate at a velocity of ~116 $\mu m \cdot s^{-1}$ for distances up to ~1 mm (Tallini et al., 2007). These intercellular waves are associated with vasodilation and are hypothesized to regulate blood flow to the parenchyma by inducing upstream dilation of arterioles (Tallini et al., 2007). The intercellular waves observed in the present study had a slower velocity (~5 to 15 $\mu m \cdot s^{-1}$) than those in mouse cremaster arterioles, suggesting a different physiological control mechanism.

In previous studies, when endothelial $IP_3R$-mediated signalling was eliminated by depletion of the internal $Ca^{2+}$ store, activation of TRPV4 channels induced a large but highly localized (few square micrometres) increase in $Ca^{2+}$ concentrations (Sonkusare et al., 2012). These localized $Ca^{2+}$ signals were reported to activate endothelial $Ca^{2+}$-activated $K^+$ channels (Sonkusare et al., 2012) and lead to endothelial hyperpolarization and vasodilation (Sonkusare et al., 2012). However, activation of TRPV4 channels is known to also control the orientation of endothelial cells, regulate endothelial permeability, and modulate the production of antithrombotic factors, each of which may require a more global $[Ca^{2+}]$ increase throughout the cytoplasm (Noren et al., 2016; Phuong et al., 2017; Thodeti et al., 2009; Thoppil et al., 2016). In the present study, $IP_3R$-mediated $Ca^{2+}$ release generated propagating $Ca^{2+}$ waves and provided a mechanism by which TRPV4 channel activity, in the presence of a functioning $Ca^{2+}$ store, may generate large rises in $Ca^{2+}$ throughout the cytoplasm. These propagating waves are critical for TRPV4-mediated control of vascular tone. When $Ca^{2+}$ release from the internal store is inhibited, TRPV4-mediated endothelial control of tone is abolished (Figure 10). This result suggests that control of vascular tone by TRPV4 channels is mediated by $Ca^{2+}$-induced $Ca^{2+}$ release via $IP_3Rs$. It is tempting to also speculate that the more general rise in $Ca^{2+}$ throughout the cells, which occurs as a result of the propagating $IP_3R$ mediated $Ca^{2+}$ waves, will facilitate TRPV4-mediated control of endothelial permeability and the production of antithrombotic factors (Noren et al., 2016; Phuong et al., 2017; Thodeti et al., 2009; Thoppil et al., 2016).

ACh evoked rapid asynchronous $Ca^{2+}$ waves in neighbouring endothelial cells. ACh-evoked changes in intracellular $Ca^{2+}$ concentration are linked closely to the $IP_3$-sensitive $Ca^{2+}$ store, but they do not involve TRPV4 channels in rat arteries (Hartmannsgruber et al., 2007; see also Kohler et al., 2006; Wilson, Lee, & McCarron, 2016; Figure 10). While the response to the activation by ACh and activation of TRPV4 channels each involved $IP_3$, the $Ca^{2+}$ signals generated had very different characteristics. ACh-evoked $Ca^{2+}$ increases did not

appear to coordinate between cells. Activation of TRPV4 channels evoked a slowly increasing baseline and large propagating $Ca^{2+}$ waves.

Endothelial TRPV4 channels are involved in several cardiovascular control mechanisms, including inhibiting vasoconstriction in small skeletal muscle arteries in response to increases in temperature (Gifford et al., 2014), regulating myogenic tone (Bagher et al., 2012), remodelling of the cytoskeleton and reorientation of the endothelial cells in response to mechanical forces (Thodeti et al., 2009), collateral vessel growth (Sayed et al., 2010; Schierling et al., 2011; Troidl et al., 2009), and arachidonic acid-induced endothelial cell migration required for angiogenesis (Fiorio Pla et al., 2012). The present results show that when the internal $IP_3$ sensitive store is intact, TRPV4 channel activity evokes $IP_3R$ signalling to generate $Ca^{2+}$ waves that propagate within and between cells, and through the $Ca^{2+}$ store, TRPV4 channels modulate vascular contractility. The results demonstrate a link between TRPV4 channel activity and $Ca^{2+}$-induced $Ca^{2+}$ release at $IP_3R$ in endothelial cells and offer a new target for drug development.

## ACKNOWLEDGEMENTS

This work was funded by the Wellcome Trust (202924/Z/16/Z and 204682/Z/16/Z) and the British Heart Foundation (PG/16/54/32230 and PG16/82/32439), whose support is gratefully acknowledged. The authors would like to thank Margaret MacDonald for her excellent technical support.

## CONFLICT OF INTEREST

The authors declare no conflicts of interest.

## AUTHOR CONTRIBUTIONS

H.R.H., M.D.L.,C.W., and J.G.M. developed the concept. H.R.H., M.D.L., X.Z., and C.W. performed the experiments. C.W. and C.D.S. wrote the analysis software. H.R.H., M.D.L., X.Z., and C.W. analysed the data. J.G.M. and H.R.H. drafted the manuscript. J.G.M., H.R.H., C.W., C.D.S., and M.D.L. edited the manuscript. J.G.M., M.D.L., C.W., and X.Z. revised the manuscript. C.W., C.D.S., and J.G.M. sourced funding. All authors approved the final version of the manuscript.

## DECLARATION OF TRANSPARENCY AND SCIENTIFIC RIGOUR

This Declaration acknowledges that this paper adheres to the principles for transparent reporting and scientific rigour of preclinical research as stated in the *BJP* guidelines for Design & Analysis and Animal Experimentation, and as recommended by funding agencies, publishers and other organisations engaged with supporting research

## DATA AVAILABILITY

All data underpinning this study is available from the authors upon reasonable request.

## ORCID

*John G. McCarron* https://orcid.org/0000-0002-3302-3984

## REFERENCES

Adkins, C. E., & Taylor, C. W. (1999). Lateral inhibition of inositol 1,4,5-trisphosphate receptors by cytosolic $Ca^{2+}$. *Current Biology*, *9*, 1115–1118. https://doi.org/10.1016/S0960-9822(99)80481-3

Aird, W. C. (2012). Endothelial cell heterogeneity. *Cold Spring Harbor Perspectives in Medicine*, *2*(1), a006429. https://doi.org/10.1101/cshperspect.a006429

Alexander, S. P. H., Christopoulos, A., Davenport, A. P., Kelly, E., Marrion, N. V., Peters, J. A., … CGTP Collaborators. (2017). The Concise Guide to PHARMACOLOGY 2017/18: G protein-coupled receptors. *British Journal of Pharmacology*, *174*, S17–S129. https://doi.org/10.1111/bph.13878

Alexander, S. P. H., Fabbro, D., Kelly, E., Marrion, N. V., Peters, J. A., Faccenda, E., … CGTP Collaborators. (2017). The Concise Guide to PHARMACOLOGY 2017/18: Enzymes. *British Journal of Pharmacology*, *174*, S272–S359. https://doi.org/10.1111/bph.13877

Alexander, S. P. H., Peters, J. A., Kelly, E., Marrion, N. V., Faccenda, E., Harding, S. D., … CGTP Collaborators. (2017). The Concise Guide to PHARMACOLOGY 2017/18: Ligand-gated ion channels. *British Journal of Pharmacology*, *174*, S130–S159. https://doi.org/10.1111/bph.13879

Alexander, S. P. H., Striessnig, J., Kelly, E., Marrion, N. V., Peters, J. A., Faccenda, E., … CGTP Collaborators. (2017). The Concise Guide to PHARMACOLOGY 2017/18: Voltage-gated ion channels. *British Journal of Pharmacology*, *174*, S160–S194. https://doi.org/10.1111/bph.13884

Bagher, P., Beleznai, T., Kansui, Y., Mitchell, R., Garland, C. J., & Dora, K. A. (2012). Low intravascular pressure activates endothelial cell TRPV4 channels, local $Ca^{2+}$ events, and IKCa channels, reducing arteriolar tone. *Proceedings of the National Academy of Sciences of the United States of America*, *109*(44), 18174–18179. https://doi.org/10.1073/pnas.1211946109

Berridge, M. J. (1997). Elementary and global aspects of calcium signalling. *The Journal of Experimental Biology*, *200*(Pt 2), 315–319.

Bootman, M., Niggli, E., Berridge, M., & Lipp, P. (1997). Imaging the hierarchical $Ca^{2+}$ signalling system in HeLa cells. *The Journal of Physiology*, *499*, 307–314. https://doi.org/10.1113/jphysiol.1997.sp021928

Bootman, M. D., Berridge, M. J., & Lipp, P. (1997). Cooking with calcium: The recipes for composing global signals from elementary events. *Cell*, *91*, 367–373. https://doi.org/10.1016/S0092-8674(00)80420-1

Borisova, L., Wray, S., Eisner, D. A., & Burdyga, T. (2009). How structure, Ca signals, and cellular communications underlie function in precapillary arterioles. *Circulation Research*, *105*(8), 803–810. https://doi.org/10.1161/CIRCRESAHA.109.202960

Catterall, W. A. (2011). Voltage-gated calcium channels. *Cold Spring Harbor Perspectives in Biology*, *3*(8), a003947. https://doi.org/10.1101/cshperspect.a003947

Cibulsky, S. M., & Sather, W. A. (1999). Block by ruthenium red of cloned neuronal voltage-gated calcium channels. *The Journal of Pharmacology and Experimental Therapeutics*, *289*(3), 1447–1453.

Dunn, K. M., Hill-Eubanks, D. C., Liedtke, W. B., & Nelson, M. T. (2013). TRPV4 channels stimulate $Ca^{2+}$-induced $Ca^{2+}$ release in astrocytic endfeet and amplify neurovascular coupling responses. *Proceedings of the National Academy of Sciences of the United States of America*, *110*(15), 6157–6162. https://doi.org/10.1073/pnas.1216514110

Earley, S., Heppner, T. J., Nelson, M. T., & Brayden, J. E. (2005). TRPV4 forms a novel $Ca^{2+}$ signaling complex with ryanodine receptors and

BKCa channels. *Circulation Research*, *97*(12), 1270–1279. https://doi.org/10.1161/01.RES.0000194321.60300.d6

Ehrlich, B. E., Kaftan, E., Bezprozvannaya, S., & Bezprozvanny, I. (1994). The pharmacology of intracellular $Ca^{2+}$-release channels. *Trends in Pharmacological Sciences*, *15*(5), 145–149. https://doi.org/10.1016/0165-6147(94)90074-4

Eilers, P. H. C., & Boelens, H. F. M. (2005). Baseline correction with asymmetric least squares smoothing. *Leiden University Medical Centre Report*.

Filosa, J. A., Yao, X., & Rath, G. (2013). TRPV4 and the regulation of vascular tone. *Journal of Cardiovascular Pharmacology*, *61*(2), 113–119. https://doi.org/10.1097/FJC.0b013e318279ba42

Fiorio Pla, A., Ong, H. L., Cheng, K. T., Brossa, A., Bussolati, B., Lockwich, T., … Ambudkar, I. S. (2012). TRPV4 mediates tumor-derived endothelial cell migration via arachidonic acid-activated actin remodeling. *Oncogene*, *31*(2), 200–212. https://doi.org/10.1038/onc.2011.231

Foskett, J. K., White, C., Cheung, K. H., & Mak, D. O. (2007). Inositol trisphosphate receptor $Ca^{2+}$ release channels. *Physiological Reviews*, *87*(2), 593–658. https://doi.org/10.1152/physrev.00035.2006

Freichel, M., Suh, S. H., Pfeifer, A., Schweig, U., Trost, C., Weissgerber, P., … Nilius, B. (2001). Lack of an endothelial store-operated $Ca^{2+}$ current impairs agonist-dependent vasorelaxation in $TRP4^{-/-}$ mice. *Nature Cell Biology*, *3*(2), 121–127. https://doi.org/10.1038/35055019

Gao, F., & Wang, D. H. (2010). Hypotension induced by activation of the transient receptor potential vanilloid 4 channels: Role of $Ca^{2+}$-activated $K^+$ channels and sensory nerves. *Journal of Hypertension*, *28*(1), 102–110. https://doi.org/10.1097/HJH.0b013e328332b865

Gao, X., Wu, L., & O'Neil, R. G. (2003). Temperature-modulated diversity of TRPV4 channel gating: Activation by physical stresses and phorbol ester derivatives through protein kinase C-dependent and -independent pathways. *The Journal of Biological Chemistry*, *278*(29), 27129–27137. https://doi.org/10.1074/jbc.M302517200

Gifford, J. R., Ives, S. J., Park, S. Y., Andtbacka, R. H., Hyngstrom, J. R., Mueller, M. T., … Richardson, R. S. (2014). α1- and α2-adrenergic responsiveness in human skeletal muscle feed arteries: The role of TRPV ion channels in heat-induced sympatholysis. *American Journal of Physiology. Heart and Circulatory Physiology*, *307*(9), H1288–H1297. https://doi.org/10.1152/ajpheart.00068.2014

Hardie, R. C., Gu, Y., Martin, F., Sweeney, S. T., & Raghu, P. (2004). In vivo light-induced and basal phospholipase C activity in Drosophila photoreceptors measured with genetically targeted phosphatidylinositol 4,5-bisphosphate-sensitive ion channels (Kir2.1). *The Journal of Biological Chemistry*, *279*(46), 47773–47782. https://doi.org/10.1074/jbc.M407525200

Harding, S. D., Sharman, J. L., Faccenda, E., Southan, C., Pawson, A. J., Ireland, S., … NC-IUPHAR. (2018). The IUPHAR/BPS guide to pharmacology in 2018: Updates and expansion to encompass the new guide to immunopharmacology. *Nucleic Acids Research*, *46*(D1), D1091–D1106. https://doi.org/10.1093/nar/gkx1121

Harraz, O. F., Longden, T. A., Hill-Eubanks, D., & Nelson, M. T. (2018). PIP2 depletion promotes TRPV4 channel activity in mouse brain capillary endothelial cells. *eLife*, *7*. https://doi.org/10.7554/eLife.38689

Hartmannsgruber, V., Heyken, W. T., Kacik, M., Kaistha, A., Grgic, I., Harteneck, C., … Köhler, R. (2007). Arterial response to shear stress critically depends on endothelial TRPV4 expression. *PLoS ONE*, *2*(9), e827. https://doi.org/10.1371/journal.pone.0000827

Hofmann, T., Schaefer, M., Schultz, G., & Gudermann, T. (2002). Subunit composition of mammalian transient receptor potential channels in living cells. *Proceedings of the National Academy of Sciences of the United States of America*, *99*(11), 7461–7466. https://doi.org/10.1073/pnas.102596199

Huang, T. Y., Chu, T. F., Chen, H. I., & Jen, C. J. (2000). Heterogeneity of $[Ca^{2+}]_i$ signaling in intact rat aortic endothelium. *The FASEB Journal*, *14*(5), 797–804. https://doi.org/10.1096/fasebj.14.5.797

Kohler, R., Heyken, W. T., Heinau, P., Schubert, R., Si, H., Kacik, M., … Hoyer, J. (2006). Evidence for a functional role of endothelial transient receptor potential V4 in shear stress-induced vasodilatation. *Arteriosclerosis, Thrombosis, and Vascular Biology*, *26*(7), 1495–1502. https://doi.org/10.1161/01.ATV.0000225698.36212.6a

Kilkenny, C., Browne, W., Cuthill, I. C., Emerson, M., & Altman, D. G. (2010). Animal research: Reporting *in vivo* experiments: The ARRIVE guidelines. *British Journal of Pharmacology*, *160*, 1577–1579.

Lawton, P. F., Lee, M. D., Saunter, C. D., Girkin, J. M., McCarron, J. G., & Wilson, C. (2019). VasoTracker, a low-cost and open source pressure myograph system for vascular physiology has been approved for production and accepted for publication in Frontiers in Physiology, section Vascular Physiology. *Frontiers in Physiology*, *10*. https://doi.org/10.3389/fphys.2019.00099

Lee, M. D., Wilson, C., Saunter, C. D., Kennedy, C., Girkin, J. M., & McCarron, J. G. (2018). Spatially structured cell populations process multiple sensory signals in parallel in intact vascular endothelium. *Science Signaling*, *11*(561), eaar4411. https://doi.org/10.1126/scisignal.aar4411

Leybaert, L., & Sanderson, M. J. (2012). Intercellular $Ca^{2+}$ waves: Mechanisms and function. *Physiological Reviews*, *92*(3), 1359–1392. https://doi.org/10.1152/physrev.00029.2011

Liedtke, W., Choe, Y., Marti-Renom, M. A., Bell, A. M., Denis, C. S., Sali, A., … Heller, S. (2000). Vanilloid receptor-related osmotically activated channel (VR-OAC), a candidate vertebrate osmoreceptor. *Cell*, *103*(3), 525–535. https://doi.org/10.1016/S0092-8674(00)00143-4

Liedtke, W., Tobin, D. M., Bargmann, C. I., & Friedman, J. M. (2003). Mammalian TRPV4 (VR-OAC) directs behavioral responses to osmotic and mechanical stimuli in *Caenorhabditis elegans*. *Proceedings of the National Academy of Sciences of the United States of America*, *100*(Suppl 2), 14531–14536. https://doi.org/10.1073/pnas.2235619100

Ma, X., Du, J., Zhang, P., Deng, J., Liu, J., Lam, F. F., … Yao, X. (2013). Functional role of TRPV4-KCa2.3 signaling in vascular endothelial cells in normal and streptozotocin-induced diabetic rats. *Hypertension*, *62*(1), 134–139. https://doi.org/10.1161/HYPERTENSIONAHA.113.01500

Macmillan, D., & McCarron, J. G. (2010). The phospholipase C inhibitor U-73122 inhibits $Ca^{2+}$ release from the intracellular sarcoplasmic reticulum $Ca^{2+}$ store by inhibiting $Ca^{2+}$ pumps in smooth muscle. *British Journal of Pharmacology*, *160*(6), 1295–1301. https://doi.org/10.1111/j.1476-5381.2010.00771.x

Mannaa, M., Marko, L., Balogh, A., Vigolo, E., N'Diaye, G., Kassmann, M., … Gollasch, M. (2018). Transient receptor potential vanilloid 4 channel deficiency aggravates tubular damage after acute renal ischaemia reperfusion. *Scientific Reports*, *8*(1), 4878. https://doi.org/10.1038/s41598-018-23165-0

Marie, I., & Beny, J. L. (2002). Calcium imaging of murine thoracic aorta endothelium by confocal microscopy reveals inhomogeneous distribution of endothelial cells responding to vasodilator agents. *Journal of Vascular Research*, *39*(3), 260–267. https://doi.org/10.1159/000063691

Marrelli, S. P., O'Neil, R. G., Brown, R. C., & Bryan, R. M. Jr. (2007). PLA2 and TRPV4 channels regulate endothelial calcium in cerebral arteries. *American Journal of Physiology. Heart and Circulatory Physiology*, *292*(3), H1390–H1397. https://doi.org/10.1152/ajpheart.01006.2006

McCarron, J. G., Chalmers, S., Bradley, K. N., Macmillan, D., & Muir, T. C. (2006). $Ca^{2+}$ microdomains in smooth muscle. *Cell Calcium*, *40*, 461–493. https://doi.org/10.1016/j.ceca.2006.08.010

McCarron, J. G., Chalmers, S., MacMillan, D., & Olson, M. L. (2010). Agonist-evoked $Ca^{2+}$ wave progression requires $Ca^{2+}$ and $IP_3$. *Journal of Cell Physiology*, *244*, 334–344.

McCarron, J. G., Lee, M. D., & Wilson, C. (2017). The endothelium solves problems that endothelial cells do not know exist. *Trends in Pharmacological Sciences*, *38*(4), 322–338. https://doi.org/10.1016/j.tips.2017.01.008

McCarron, J. G., MacMillan, D., Bradley, K. N., Chalmers, S., & Muir, T. C. (2004). Origin and mechanisms of $Ca^{2+}$ waves in smooth muscle as revealed by localized photolysis of caged inositol 1,4,5-trisphosphate. *The Journal of Biological Chemistry*, *279*, 8417–8427. https://doi.org/10.1074/jbc.M311797200

McCarron, J. G., Wilson, C., Heathcote, H. R., Zhang, X., Buckley, C., & Lee, M. D. (2019). Heterogeneity and emergent behaviour in the vascular endothelium. *Current Opinion in Pharmacology*, *45*, 23–32. https://doi.org/10.1016/j.coph.2019.03.008

Mendoza, S. A., Fang, J., Gutterman, D. D., Wilcox, D. A., Bubolz, A. H., Li, R., … Zhang, D. X. (2010). TRPV4-mediated endothelial $Ca^{2+}$ influx and vasodilation in response to shear stress. *American Journal of Physiology. Heart and Circulatory Physiology*, *298*(2), H466–H476. https://doi.org/10.1152/ajpheart.00854.2009

Mizuno, A., Matsumoto, N., Imai, M., & Suzuki, M. (2003). Impaired osmotic sensation in mice lacking TRPV4. *American Journal of Physiology. Cell Physiology*, *285*(1), C96–C101. https://doi.org/10.1152/ajpcell.00559.2002

Moccia, F., Berra-Romani, R., & Tanzi, F. (2012). Update on vascular endothelial $Ca^{2+}$ signalling: A tale of ion channels, pumps and transporters. *World Journal of Biological Chemistry*, *3*(7), 127–158. https://doi.org/10.4331/wjbc.v3.i7.127

Moore, C., Cevikbas, F., Pasolli, H. A., Chen, Y., Kong, W., Kempkes, C., … Liedtke, W. B. (2013). UVB radiation generates sunburn pain and affects skin by activating epidermal TRPV4 ion channels and triggering endothelin-1 signaling. *Proceedings of the National Academy of Sciences of the United States of America*, *110*(34), E3225–E3234. https://doi.org/10.1073/pnas.1312933110

Mumtaz, S., Burdyga, G., Borisova, L., Wray, S., & Burdyga, T. (2011). The mechanism of agonist induced $Ca^{2+}$ signalling in intact endothelial cells studied confocally in in situ arteries. *Cell Calcium*, *49*(1), 66–77. https://doi.org/10.1016/j.ceca.2010.11.010

Nelson, M. T., Patlak, J. B., Worley, J. F., & Standen, N. B. (1990). Calcium channels, potassium channels, and voltage dependence of arterial smooth muscle tone. *The American Journal of Physiology*, *259*(1 Pt 1), C3–C18. https://doi.org/10.1152/ajpcell.1990.259.1.C3

Nilius, B., Droogmans, G., & Wondergem, R. (2003). Transient receptor potential channels in endothelium: Solving the calcium entry puzzle? *Endothelium: Journal of Endothelial Cell Research*, *10*(1), 5–15. https://doi.org/10.1080/10623320303356

Nilius, B., & Voets, T. (2013). The puzzle of TRPV4 channelopathies. *EMBO Reports*, *14*(2), 152–163. https://doi.org/10.1038/embor.2012.219

Nilius, B., Watanabe, H., & Vriens, J. (2003). The TRPV4 channel: Structure–function relationship and promiscuous gating behaviour. *Pflügers Archiv*, *446*(3), 298–303. https://doi.org/10.1007/s00424-003-1028-9

Noren, D. P., Chou, W. H., Lee, S. H., Qutub, A. A., Warmflash, A., Wagner, D. S., … Levchenko, A. (2016). Endothelial cells decode VEGF-mediated $Ca^{2+}$ signaling patterns to produce distinct functional responses. *Science Signaling*, *9*(416), ra20. https://doi.org/10.1126/scisignal.aad3188

Oancea, E., & Meyer, T. (1996). Reversible desensitization of inositol trisphosphate-induced calcium release provides a mechanism for repetitive calcium spikes. *The Journal of Biological Chemistry*, *271*, 17253–17260. https://doi.org/10.1074/jbc.271.29.17253

Olson, M. L., Chalmers, S., & McCarron, J. G. (2012). Mitochondrial organization and $Ca^{2+}$ uptake. *Biochemical Society Transactions*, *40*(1), 158–167. https://doi.org/10.1042/BST20110705

Olson, M. L., Sandison, M. E., Chalmers, S., & McCarron, J. G. (2012). Microdomains of muscarinic acetylcholine and $Ins(1,4,5)P_3$ receptors create '$Ins(1,4,5)P_3$ junctions' and sites of $Ca^{2+}$ wave initiation in smooth muscle. *Journal of Cell Science*, *125*(Pt 22, 5315–5328. https://doi.org/10.1242/jcs.105163

Parker, I., & Ivorra, I. (1991). Caffeine inhibits inositol trisphosphate-mediated liberation of intracellular calcium in Xenopus oocytes. *The Journal of Physiology*, *433*, 229–240. https://doi.org/10.1113/jphysiol.1991.sp018423

Peppiatt, C. M., Collins, T. J., Mackenzie, L., Conway, S. J., Holmes, A. B., Bootman, M. D., … Roderick, H. L. (2003). 2-Aminoethoxydiphenyl borate (2-APB) antagonises inositol 1,4,5-trisphosphate-induced calcium release, inhibits calcium pumps and has a use-dependent and slowly reversible action on store-operated calcium entry channels. *Cell Calcium*, *34*(1), 97–108. https://doi.org/10.1016/S0143-4160(03)00026-5

Phuong, T. T. T., Redmon, S. N., Yarishkin, O., Winter, J. M., Li, D. Y., & Krizaj, D. (2017). Calcium influx through TRPV4 channels modulates the adherens contacts between retinal microvascular endothelial cells. *The Journal of Physiology*, *595*(22), 6869–6885. https://doi.org/10.1113/JP275052

Running Deer, J. L., Hurley, J. B., & Yarfitz, S. L. (1995). G protein control of Drosophila photoreceptor phospholipase C. *The Journal of Biological Chemistry*, *270*(21), 12623–12628. https://doi.org/10.1074/jbc.270.21.12623

Rusko, J., Wang, X., & Vanbreemen, C. (1995). Regenerative caffeine-induced responses in native rabbit aortic endothelial-cells. *British Journal of Pharmacology*, *115*(5), 811–821. https://doi.org/10.1111/j.1476-5381.1995.tb15005.x

Saleem, H., Tovey, S. C., Molinski, T. F., & Taylor, C. W. (2014). Interactions of antagonists with subtypes of inositol 1,4,5-trisphosphate (IP3) receptor. *British Journal of Pharmacology*, *171*(13), 3298–3312. https://doi.org/10.1111/bph.12685

Sayed, A., Schierling, W., Troidl, K., Ruding, I., Nelson, K., Apfelbeck, H., … Schmitz-Rixen, T. (2010). Exercise linked to transient increase in expression and activity of cation channels in newly formed hind-limb collaterals. *European Journal of Vascular and Endovascular Surgery*, *40*(1), 81–87. https://doi.org/10.1016/j.ejvs.2010.02.014

Schierling, W., Troidl, K., Apfelbeck, H., Troidl, C., Kasprzak, P. M., Schaper, W., & Schmitz-Rixen, T. (2011). Cerebral arteriogenesis is enhanced by pharmacological as well as fluid-shear-stress activation of the Trpv4 calcium channel. *European Journal of Vascular and Endovascular Surgery*, *41*(5), 589–596. https://doi.org/10.1016/j.ejvs.2010.11.034

Shen, J., Tu, L., Chen, D., Tan, T., Wang, Y., & Wang, S. (2018). TRPV4 channels stimulate $Ca^{2+}$-induced $Ca^{2+}$ release in mouse neurons and trigger endoplasmic reticulum stress after intracerebral hemorrhage. *Brain Research Bulletin*, *146*, 143–152.

Sonkusare, S. K., Bonev, A. D., Ledoux, J., Liedtke, W., Kotlikoff, M. I., Heppner, T. J., … Nelson, M. T. (2012). Elementary $Ca^{2+}$ signals through endothelial TRPV4 channels regulate vascular function. *Science*, *336*(6081), 597–601. https://doi.org/10.1126/science.1216283

Sonkusare, S. K., Dalsgaard, T., Bonev, A. D., Hill-Eubanks, D. C., Kotlikoff, M. I., Scott, J. D., … Nelson, M. T. (2014). AKAP150-dependent cooperative TRPV4 channel gating is central to endothelium-dependent vasodilation and is disrupted in hypertension. *Science Signaling*, *7*(333), ra66. https://doi.org/10.1126/scisignal.2005052

Strotmann, R., Schultz, G., & Plant, T. D. (2003). $Ca^{2+}$-dependent potentiation of the nonselective cation channel TRPV4 is mediated by a C-terminal calmodulin binding site. *The Journal of Biological Chemistry*, *278*(29), 26541–26549. https://doi.org/10.1074/jbc.M302590200

Sullivan, M. N., Francis, M., Pitts, N. L., Taylor, M. S., & Earley, S. (2012). Optical recording reveals novel properties of GSK1016790A-induced vanilloid transient receptor potential channel TRPV4 activity in primary human endothelial cells. *Molecular Pharmacology*, *82*(3), 464–472. https://doi.org/10.1124/mol.112.078584

Sun, M. Y., Geyer, M., & Komarova, Y. A. (2017). IP3 receptor signaling and endothelial barrier function. *Cellular and Molecular Life Sciences*, *74*(22), 4189–4207. https://doi.org/10.1007/s00018-017-2624-8

Tallini, Y. N., Brekke, J. F., Shui, B., Doran, R., Hwang, S. M., Nakai, J., … Kotlikoff, M. I. (2007). Propagated endothelial $Ca^{2+}$ waves and arteriolar dilation in vivo: measurements in Cx40BAC GCaMP2 transgenic mice. *Circulation Research*, *101*(12), 1300–1309. https://doi.org/10.1161/CIRCRESAHA.107.149484

Taylor, M. S., Bonev, A. D., Gross, T. P., Eckman, D. M., Brayden, J. E., Bond, C. T., … Nelson, M. T. (2003). Altered expression of small-conductance $Ca^{2+}$-activated $K^+$ (SK3) channels modulates arterial tone and blood pressure. *Circulation Research*, *93*(2), 124–131. https://doi.org/10.1161/01.RES.0000081980.63146.69

Thodeti, C. K., Matthews, B., Ravi, A., Mammoto, A., Ghosh, K., Bracha, A. L., & Ingber, D. E. (2009). TRPV4 channels mediate cyclic strain-induced endothelial cell reorientation through integrin-to-integrin signaling. *Circulation Research*, *104*(9), 1123–1130. https://doi.org/10.1161/CIRCRESAHA.108.192930

Thoppil, R. J., Cappelli, H. C., Adapala, R. K., Kanugula, A. K., Paruchuri, S., & Thodeti, C. K. (2016). TRPV4 channels regulate tumor angiogenesis via modulation of Rho/Rho kinase pathway. *Oncotarget*, *7*(18), 25849–25861. https://doi.org/10.18632/oncotarget.8405

Trebak, M., Bird, G. S., McKay, R. R., & Putney, J. W. Jr. (2002). Comparison of human TRPC3 channels in receptor-activated and store-operated modes. Differential sensitivity to channel blockers suggests fundamental differences in channel composition. *Journal of Biological Chemistry*, *277*(24), 21617–21623. https://doi.org/10.1074/jbc.M202549200

Troidl, C., Troidl, K., Schierling, W., Cai, W. J., Nef, H., Mollmann, H., … Schaper, W. (2009). Trpv4 induces collateral vessel growth during regeneration of the arterial circulation. *Journal of Cellular and Molecular Medicine*, *13*(8B), 2613–2621. https://doi.org/10.1111/j.1582-4934.2008.00579.x

Voets, T., Prenen, J., Fleig, A., Vennekens, R., Watanabe, H., Hoenderop, J. G., … Nilius, B. (2001). CaT1 and the calcium release-activated calcium channel manifest distinct pore properties. *The Journal of Biological Chemistry*, *276*(51), 47767–47770. https://doi.org/10.1074/jbc.C100607200

Vriens, J., Watanabe, H., Janssens, A., Droogmans, G., Voets, T., & Nilius, B. (2004). Cell swelling, heat, and chemical agonists use distinct pathways for the activation of the cation channel TRPV4. *Proceedings of the National Academy of Sciences of the United States of America*, *101*(1), 396–401. https://doi.org/10.1073/pnas.0303329101

Watanabe, H., Davis, J. B., Smart, D., Jerman, J. C., Smith, G. D., Hayes, P., … Nilius, B. (2002). Activation of TRPV4 channels (hVRL-2/mTRP12) by phorbol derivatives. *The Journal of Biological Chemistry*, *277*(16), 13569–13577. https://doi.org/10.1074/jbc.M200062200

Watanabe, H., Vriens, J., Janssens, A., Wondergem, R., Droogmans, G., & Nilius, B. (2003). Modulation of TRPV4 gating by intra- and extracellular $Ca^{2+}$. *Cell Calcium*, *33*(5–6), 489–495. https://doi.org/10.1016/S0143-4160(03)00064-2

Watanabe, H., Vriens, J., Prenen, J., Droogmans, G., Voets, T., & Nilius, B. (2003). Anandamide and arachidonic acid use epoxyeicosatrienoic acids to activate TRPV4 channels. *Nature*, *424*(6947), 434–438. https://doi.org/10.1038/nature01807

Whorton, A. R., Willis, C. E., Kent, R. S., & Young, S. L. (1984). The role of calcium in the regulation of prostacyclin synthesis by porcine aortic endothelial cells. *Lipids*, *19*(1), 17–24. https://doi.org/10.1007/BF02534603

Willars, G. B., Nahorski, S. R., & Challiss, R. A. (1998). Differential regulation of muscarinic acetylcholine receptor-sensitive polyphosphoinositide pools and consequences for signaling in human neuroblastoma cells. *The Journal of Biological Chemistry*, *273*(9), 5037–5046. https://doi.org/10.1074/jbc.273.9.5037

Wilson, C., Lee, M., & McCarron, J. G. (2016). Acetylcholine released by endothelial cells facilitates flow-mediated dilatation. *The Journal of Physiology*, *594*, 7267–7307. https://doi.org/10.1113/JP272927

Wilson, C., Lee, M. D., Heathcote, H. R., Zhang, X., Buckley, C., Girkin, J. M., … McCarron, J. G. (2019). Mitochondrial ATP production provides long-range control of endothelial inositol trisphosphate-evoked calcium signaling. *The Journal of Biological Chemistry*, *294*(3), 737–758. https://doi.org/10.1074/jbc.RA118.005913

Wilson, C., Saunter, C. D., Girkin, J. M., & McCarron, J. G. (2015). Pressure-dependent regulation of $Ca^{2+}$ signaling in the vascular endothelium. *The Journal of Physiology*, *593*, 5231–5253. https://doi.org/10.1113/JP271157

Wilson, C., Saunter, C. D., Girkin, J. M., & McCarron, J. G. (2016). Clusters of specialized detector cells provide sensitive and high fidelity receptor signaling in intact endothelium. *The FASEB Journal*, *30*, 2000–2013. https://doi.org/10.1096/fj.201500090

Yin, J., Hoffmann, J., Kaestle, S. M., Neye, N., Wang, L., Baeurle, J., … Kuebler, W. M. (2008). Negative-feedback loop attenuates hydrostatic lung edema via a cGMP-dependent regulation of transient receptor potential vanilloid 4. *Circulation Research*, *102*(8), 966–974. https://doi.org/10.1161/CIRCRESAHA.107.168724

Zhang, D. X., Mendoza, S. A., Bubolz, A. H., Mizuno, A., Ge, Z. D., Li, R., … Gutterman, D. D. (2009). Transient receptor potential vanilloid type 4-deficient mice exhibit impaired endothelium-dependent relaxation induced by acetylcholine in vitro and in vivo. *Hypertension*, *53*(3), 532–538. https://doi.org/10.1161/HYPERTENSIONAHA.108.127100

Zhang, L., Papadopoulos, P., & Hamel, E. (2013). Endothelial TRPV4 channels mediate dilation of cerebral arteries: Impairment and recovery in cerebrovascular pathologies related to Alzheimer's disease. *British Journal of Pharmacology*, *170*(3), 661–670. https://doi.org/10.1111/bph.12315

## SUPPORTING INFORMATION

Additional supporting information may be found online in the Supporting Information section at the end of the article.

**How to cite this article:** Heathcote HR, Lee MD, Zhang X, Saunter CD, Wilson C, McCarron JG. Endothelial TRPV4 channels modulate vascular tone by $Ca^{2+}$-induced $Ca^{2+}$ release at inositol 1,4,5-trisphosphate receptors. *Br J Pharmacol*. 2019;176:3297–3317. https://doi.org/10.1111/bph.14762